STUDY ON THE CHARACTERISTIC EMISSION LOADING FROM THE PUBLIC TRANSPORT AND ITS CONTRIBUTION FOR AIR QUALITY DEGRADATION OVER THE KATHMANDU VALLEY: GRIDED EMISSION ESTIMATION AND DISPERSION MODELING

A Dissertation

Submitted to the Central Department of Physics,
Tribhuvan University, Kirtipur in the Partial Fulfilment for the Requirement of
Master's Degree of Science in Physics

By

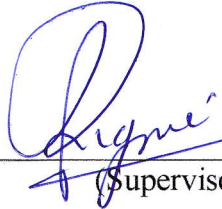## Chiranjibi Shrestha

**Roll No.: 1531/2073**

May 2021

RECOMMENDATION

It is to certify that Mr. **Chiranjibi Shrestha** has carried out the dissertation entitled **"STUDY ON THE CHARACTERISTIC EMISSION LOADING FROM THE PUBLIC TRANSPORT AND ITS CONTRIBUTION FOR AIR QUALITY DEGRADATION OVER THE KATHMANDU VALLEY: GRIDED EMISSION ESTIMATION AND DISPERSION MODELING"** under our supervision and guidance.

We recommend the project work in the partial fulfilment for the requirement of Master's Degree of science in Physics at Tribhuvan University.

(Supervisor)

Ram Prasad Regmi, PhD
Professor
Central Department of Physics,
Tribhuvan University,
Kirtipur, Kathmandu, Nepal
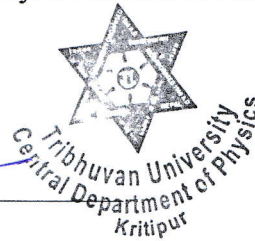
(Co-supervisor)

Mrs. Sangeeta Maharjan
Assistant
Central Department of Physics,
Tribhuvan University,
Kirtipur, Kathmandu, Nepal

Date: 9 Aug 2021

Date: 9 August 2021

ACKNOWLWDGEMENTS

EVALUATION

We certify that we have evaluated this dissertation submitted by **Mr. Chiranjibi Shrestha** entitled **"Study on the Characteristic Emission Loading from the Public Transport and its Contribution for Air Quality Degradation over the Kathmandu Valley: Gridded Emission Estimation and Dispersion Modelling"**. In our opinion, it fulfills all the specified criteria, in the scope and quality, as a dissertation for the partial fulfillment of the requirement for the Master's Degree of Science in Physics at Tribhuvan University, Kirtipur, Nepal.

Evaluation Committee

....
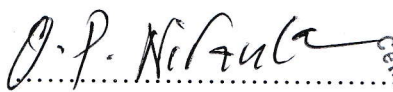
Prof. Dr. Ram Prasad Regmi

(Supervisor)

Central Department of Physics,

Tribhuvan University, Kirtipur,

Kathmandu, Nepal

....

Prof. Dr. Om Prakash Niraula

(Head of Department)

Central Department of Physics,
Tribhuvan University, Kirtipur,

Kathmandu, Nepal

....

Prof. Dr. Khem Narayan Poudyal

(External Examiner)

Department of Applied sciences,
Central Campus, Pulchowk,

Institute of Engineering, Tribhuvan
University, Lalitpur, Nepal

Date: ..28...August....2021................

....

Mrs. Sangeeta Maharjan

(Co-supervisor)

Teaching assistant

Central Department of Physics

Tribhuvan University,
Kirtipur,

Kathmandu, Nepal

....

Asso. Prof. Dr. Gopi Chandra Kafle

(Internal Examiner)

Central Department of Physics,

Tribhuvan University, Kirtipur,

Kathmandu, Nepal

ABSTRACT

The Kathmandu valley is witnessing an extremely poor air quality from years. The degradation of air quality over Kathmandu is often found to be associated with the spontaneous urbanization, haphazard industrial expansions and vehicular fleet. Present study was conceived to understand the contribution of transport sector in degrading the air quality of Kathmandu valley. We developed a comprehensive gridded emission inventories of potential pollutants and performed particulate pollutant dispersion modelling using a comprehensive Chemical Transport Modelling (CTM) at the horizontal grid resolution of 1 km^2 over an area of 70 km x 70 km that covers the Kathmandu valley and its immediate surroundings, initialized with the Weather Research and Forecasting (WRF) simulated meteorological fields.

The gridded emission inventory showed about 1918.17 kg km^{-2} of TSP, 12872.74 kg km^{-2} of CO, 6925.82 kg km^{-2} of NO_x and 708.41 kg km^{-2} of SO_2 are currently loaded into the atmosphere of the valley per day from the public transport over the Kathmandu valley. CTM simulation shows the ambient concentration of $PM_{2.5}$ due to public transport fleets appears a minimum during the day time and remains maximum during the night and morning times. The pollutants released over the valley are transported to the east and are flushed out into the eastern neighbouring valley. The contribution of the public transport fleet to the deterioration of ambient air quality of the valley appears significant compared to total emission from transport sector.

CONTENT

LIST OF FIGURES

List of tables

Acronyms and Abbreviations

ABC	Atmospheric Brown Cloud
ABL	Atmospheric Boundary Layer
AGL	Above Ground Level
AMSL	Above the Mean Sea Level
ARW	Advance Research WRF
BC	Black Carbon
CBS	Central Bureau of Statistic
NH_3	Ammonia
NMVOC	Non-Methane Volatile Organic compound
SO_x	Oxides of Sulphur
NO_x	Oxide of Nitrogen
NWP	Numerical weather prediction
OC	Organic Carbon
TSP	Total Suspended Particle
CTM	Chemical Transport Model
GIS	Geographical Information System
ICIMOD	International Center for Mountain Development
Kg	Kilogram
LPG	Liquefied Petroleum gas
LST	Local Standard Time
MMM	Mesoscale and Microscale Meteorology

NCAR	National Center For Atmospheric Research
USGS	United States Geological Survey
NCEP	National Center for Environmental Prediction
NWP	Numerical Weather Prediction
PM	Particulate Matter
RASS	Radio Acoustic Sounding System
SODAR	Sonic Detection and Ranging
Mg	Microgram
WHO	World Health Organization
GIS	Geographical Information System
WARM	Waste Reduction Model

Chapter 1
INTRODUCTION

1.1 Background of Dissertation

With the concentrated development and increasing urban density, the traffic congestion in Kathmandu valley has been increasing tremendously. These vehicles emit carbon dioxide, carbon monoxide, volatile organic compounds, nitrogen oxides, hydrocarbons and particulate matters, degrading the air quality. These days two wheelers are getting popular in Kathmandu valley. However, majority of people in the valley still depend on public transportation for daily transportation with in the valley. Besides, public transportations are good mode of transportation to transfer large commuters to long distance to and from the valley [1]. The valley hosts large number of small and large public vehicles that are barely conditioned and run in the poorly maintained roads of the Kathmandu valley. Unscientific and unmanaged public transport system is one of the main reason for traffic hustle in the valley that has contributed to the pollution in the valley. As such, the developing cities are confronted with a great challenge of controlling the atmospheric pollution, especially in rapid growing urban centres.

Air pollution has become the major problem of urban cities. The concern about air pollution continues to receive a great deal of interest worldwide due to its negative impacts on environment and climate change and on human health and welfare. Thus, there is need to curb increasing levels of air pollution for sustainable future of new generations.

Figure 1.1: Figures showing (a) traffic jam in the Kathmandu valley and (b) passengers travelling with the public transport.

This research help understand wintertime wind flows over Kathmandu valley and meteorological conditions to favor the emission loading. Likewise, the contribution of public vehicle in emitting various harmful gases in air and their dispersion over the Kathmandu valley and its surrounding areas in wintertime.

1.2 Motivation and Purpose

In consideration with the necessity of Public Transport for systematic city and economics associated with it, effective public transport is essential for the convince of public life. Considering, the fragile landscape, the delicately balanced ecosystem of the city and the public health outcome that results from increasing a Public Transport, it is imperative that increasing and developing Public Transports those are friendly to the prevailing landscape, ecosystem, and the human health. The impact of increasing or developing the public transport is determined by technology used, the location of Public Transport and the prevailing meteorological situations in and around the location of Public Transport way. An unmanaged Public Transports can have unexpectedly negative impacts on the stability of the landscape, local and regional ecosystem and the air quality and hence the human, animal and vegetation health. Present study aims to address one of the major environment issues, the impact of Public Transport to deteriorate air quality over the Kathmandu Valley.

Figure 1.2: An attempt to make people aware of air pollution in the Kathmandu valley [2]

Regmi, et al. [2, 4] The prevailing meteorological situations over such valley shaped terrains, in general, have been found to be highly unfavourable with respect to air pollution. The winds are generally directed along the valley axis, the near surface atmosphere remains strongly stratified, only limited boundary layer or mixing layer heights in excess to the carrying capacity, typically. Determined by the prevailing meteorological situation, may lead to building up of air pollution levels affecting the ecosystem, human health and vegetation of the area.

It was thus very important to understand the emissions activities over the Kathmandu Valley, meteorological situation over the region and the air pollution dispersion pattern of the pollutant released by the Public Transport for increasing an air pollution control system for the sustainable future of the area ensuring the good public health, protecting the ecosystem of the area and to create a healthy environment, manage urban city in and around the conservation area. Finding of the present research are expected to have significant applications to realize the sustainable development and managed city over the area. Moreover, several Public Transport are coming up in and around the same area without proper environmental impact assessment. It is thus very high time to have the proposed study. To the best of our knowledge, no systematic studies with this prospect have been carried out over the area.

Figure 1.3: A view of the Kathmandu valley following a day of rainfall, looking towards the North [3]

1.3 General geographical and meteorological features of the study area

Kathmandu Valley is one of the largest city which located at Bagmati province, within 27.27 degrees north (latitude) and 85.3 degrees east (longitude), at an elevation of about 1350 meters above mean see level (AMSL). The bowl-shaped Kathmandu Valley lies in the middle hills of the Central Nepal Himalaya, surrounded by steep rising mountains ranging from 500m to 1500m above the flat basin floor over the valley, with an area of approximately 570 square kilometres The valley possesses mountain passes in the western (Thankot, Bhimdhunga) and eastern (Banepa, Sanga, Nagarkot) boundaries, along with the river gorge of the Bagmati in the southwest rim of the valley. The opening connected with the valley may drive a gentle plane-to-plateau and valley wind systems. It consists of three distinct districts, namely, Kathmandu, Bhaktapur and Lalitpur. It behaves as plateau during the daytime by transporting the regional air masses up into the valley while as elevated basin by creating a deep calm cold air pool during the night period [4]. Thus, the meteorological flows associated with this valley can be projected to be complex enough. The Kathmandu valley with bowl-shaped, therefore, can be considered to exhibit an elevated basin and a plateau with a rim a rarely reported behaviour [4].

Kathmandu valley is surrounded by Mt. phulchoki in the southeast, Mt. Shivpuri in the north, Mt. Champadevi in the southwest, and Mt. Nagarjun in west whereas the central part of the valley is largely flat. The valley has a narrow river gorge in the southwest and a few low mountain passes in the western and eastern edges of the valley.

The climate of the bowl-shaped Valley is considered to be temperate sub-tropical in type. The temperature with range is below 0^0c in winter and reaches more than 30^0c in summer. The bowl-shaped valley experiences four distinct season: pre-season, monsoon, post-monsoon and winter. The rainy season is from June to September when 80% of the rainfall occurs. The mean annual rainfall and temperature are 1454 mm and 19.7^0c, respectively [5]

The prominent winds system which intrudes in the bowl-shaped valley has been identified as the relatively cooler south-westerly that usually enters into the valley through the Bagmati River gorge located in the southwest the warmer north-westerly that enters from the western low- mountain passes. They merge into a westerly over the centre of the valley and pass into a neighbouring valley via the eastern Sanga- nala passes [4]. The adverse meteorological conditions associated with the complex topography of the valley traps the pollutants within the very shallow layer and hence build up high concentration close to the surface [6].
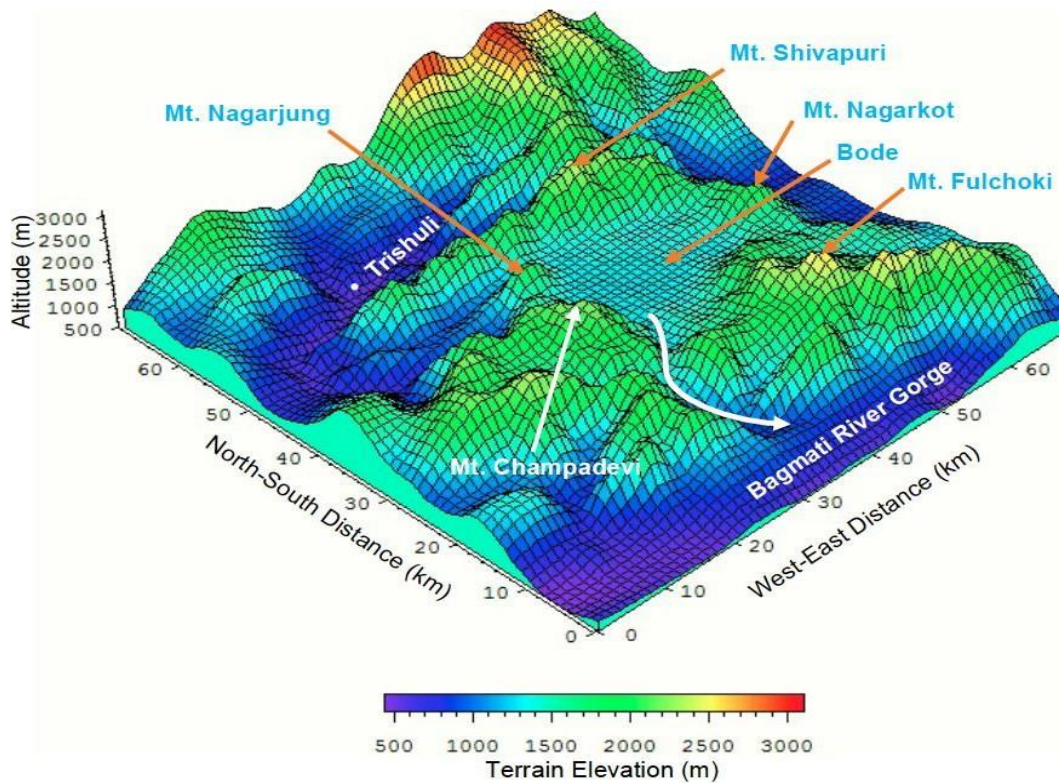
Figure 1.4: 3-D terrain structure of the Kathmandu valley and its surrounding   (Using ArcGIS 10.6)

1.4 Objectives of the study

The general objective of this study is to make a detailed study of air pollution emissions from the public transport and environmental impacts of pollutants. The proposed research aim to achieve the following specific objectives:

1.   To understand, model and predict the characteristics of meteorological flow field and their implications for air pollution transport.

2.   To prepare the gridded emission inventory of the pollutant released from the public transportation.

3.   To prepare the air pollution dispersion map emitted by public transportation.

1.5 Structure of the Dissertation

The dissertation consists of five different chapters. These chapters are further divided into several sections and subsections for their broad description.

Chapter 1: This chapter describes brief introduction on air pollution, along with the geographical and meteorological features of Kathmandu Valley. It also includes the motivational background and the objectivity of conducting the research.

Chapter 2: This chapter includes past studies on air pollution, environmental consequences of Kathmandu Valley brief introduction to key pollutions, meteorological parameters, wind system and atmosphere boundary layer.

Chapter 3: This chapter includes the methodologies adopted for this study are described with a brief overview of the dispersion modelling, and model setup and initialization of CTM.

Chapter 4: This chapter includes the simulation results of the various meteorological phenomenon using CTM and model along with their brief description.

Chapter 5: This chapter generalizes the simulation results and provides conclusions and suggestions to be employed as an outcome of the generalized result.

Chapter 6: This chapter includes the limitation of the study are described with a brief overview of the dissertation.

Chapter 2

LITERATURE REVIEW

2.1 Overview of Past studies on air pollution of Nepal

Studies of the air pollution dispersion modeling and control system development for emission over the Kathmandu valley and Lumbini region by Regmi et.al [7] strongly suggested that the National ambient air quality standard can be met by limiting the emissions from transport emission to 30% of current emissions over the Kathmandu valley and 50% for Lumbini region [7]. The investigation of human-air pollution exposure status displayed a staggering number of more than 52 percent of total Kathmandu resident were living in the areas with particulate pollutant concentration of aerodynamic size less than 10 micrometer (PM_{10}) above 40 micrograms per cubic meter. With such big numbers, an alarm was already released but no firm changes have been implemented as yet. The study showed that the SO_2 level was high in the Kathmandu valley also due to reason of public transport [7]. PM_{10} concentration was high and is the major air pollutant causing human health impact. The air pollution may cause serious damage of environmental landscape of the place which creates the problems in attainment of the environmental sustainability.

But large number of researches have been conducted within the past few years when the health specialists and environmentalists understood its adverse impacts on health and environment. In Nepal a very few researches have been carried out on air pollution activities and their impacts on human health and environment. For example Saud and Paudel (2018) have studied about the threat of Ambient air pollution in Kathmandu, Nepal. They found that air pollution has been major indicator for chronic disease like as lung disease, heart disease and cancer. Air pollution also invite respiratory diseases and allergy [8]. Also studies road transport by Shrestha, he says large energy consume by road transport at Nepal and he found CO_2 and SO_2 emission was estimated to be around 2679.4 thousand tones and vary from 4747 to 6593 tones [9].

Studies by Kitada and Regmi [10] revealed that the bowl shaped Kathmandu valley possesses high air pollution particularly during winter season because of its adverse meteorological and topographic conditions. Emission of about 2147 and 3859 Metric tons of NO_X and SO_2 respectively ,were

estimated to be loaded in the Kathmandu valley in the year 2001 [10]. Recent study on the vehicle fleet in the Kathmandu valley using International Vehicle Emission (IVE) by Shrestha et al. [11] showed that diurnal variation of emission were consistent with vehicle density and 31, 7.7, 16, 4.7, 2.1 and 1554 Gg of CO, VOC, NOx, PM, BC and CO_2 were emitted daily in the year 2010. I justified that public transport is the most important indicator in terms of the key environmental issues for has significant emissions of particulates in the Kathmandu valley. Though, the study is quite rigorous the contribution of public transportation has not been analyzed. So it becomes obvious to emphasize to study the characteristic emission loading from public transport and its contribution for air quality degradation to develop efficient control mechanism to control air pollution over the Kathmandu valley.

Table 2.1: Number of four wheel vehicle

Year	Bus	Car/Jeep	Pickup
73/74	5342	21292	10675
74/75	2972	24338	10342
75/76	2354	17953	6987
Total	49318	237658	55973
Bagmati 74/75	833	14452	3177

2.2 Air Quality Guidelines

The World Health organization (WHO) air quality guidelines have been developed to support action to achieve safety air quality level that protects public health.

The limiting values of pollutants as indicated are based on scientific evidences and the health consequences.

Table 2.2 a): World Health Organization (WHO) Air Quality Guidelines [12]

S. No.	Pollutants	Concentration
1	PM_{25}	10 µg/m^3 annual mean

		$25 \, \mu g/m^3$ annual mean
2	PM_{10}	$20 \mu g/m^3$ annual mean
		$50 \, \mu g/m^3$ annual mean
3	SO_2	$20 \, \mu g/m^3$ annual mean
		$50 \, \mu g/m^3$ annual mean
4	NO_2	$40 \, \mu g/m^3$ annual mean
		$200 \, \mu g/m^3$ annual mean
5	O_3	$100 \, \mu g/m^3$ annual mean

Now a days, Nepal's Government devoted to new standard policy for improve air Pollution. Which was represented from 2003 and standardized in 2012 (Table 2.2 b).

Table 2.2 b): National Ambient Air Quality Standard, 2012 [13].

Concentration in Ambient Air, Maximum			
Parameters	Average Timing	National Standards	WHO Standards
(Total Suspended Particles) TSP	Annual	-	-
	24-Hour	230	-
PM_{10}	Annual	-	20
	24-Hour	120	50
PM_{25}	24-Hour	40	10

Sulfur Dioxide (SO$_2$)	Annual	50	20.96
	24-Hour	70	-
Nitrogen Dioxide (NO$_2$)	Annual	40	39.48
	24-Hour	80	-
(Carbon Monoxide) CO	8-Hour	10,000	10,305
Lead	Annual	0.5	0.5
Benzene	Annual	20	-
Ozone	8-Hour	157	100

2.3 Emission Inventory of Kathmandu Valley

The Kathmandu valley is a bowl-shaped valley that consist of three cities Kathmandu valley viz. the capital city of Nepal, Lalitpur and Bhaktapur has large population boom and haphazard urbanization in recent time. With its ever increasing population and subsequent increase in Vehicles, industries, construction and commercial activities energy demand has surged up. Plentiful energy consumption is fulfilled by fossil fuel that has resulted in increase in the air pollution to unacceptable level affecting life of the people, beauty of the city and its heritage.

Table 2.3: Total estimated sectoral emission of NO$_x$, SO$_x$, CO & TSP in Kathmandu valley and its Surroundings [7]

Source	NO$_x$	SO$_x$	CO	TSP	Total
Domestic	11.44	6.79	260.57	82.13	360.94
Transport	19.11	3.82	375.13	20.29	418.35

Industry	3.35	8.14	20.56	23.60	55.63
Total	33.90	18.74	656.26	126.01	834.92

Water and Energy Commission Secretariat WECS (2010) says 89.1% total energy consumed by residential, 5.9% by transport, 3.3% by industrial, 1.3% by commercial in Nepal and remaining by agriculture and other sector of which 86% of the energy in the residential sector is supplied by fuelwood alone whereas alternative renewable energy sources fulfill hardly 1% of the energy consumed. Likewise, electricity shares 23.2%, 11% and 4.8% of industrial, commercial and agricultural sector energy need respectively and the rest is fulfilled by fossil fuels especially coal (57.7%) in industrial sector. Similarly, transportation sector also almost completely depend on petroleum. These statistics highlight our dependence in traditional/fossil fuels for energy that has resulted increased level of pollution in different urban centers in Nepal including the Kathmandu valley.

The bowl shaped valley suffered to much level of air pollution during winter season. This time emission contribution from each of the sector considered during the study has been presented in Table 2.3. Emission from each of the sector findings, total average approach of about 33. 90 tons of NO_x, 18.74 tons of SO_x, 656.26 tons of CO and 126.01 tons of TSP are emitted per day during the winter season in the Kathmandu valley and its surroundings.

The total sectorial estimated emission from transport with sum of about 418.35 tons per day (TPD), then domestic (360.94 TPD) and industrial (55.65 TPD). The relative contribution of each the sectors has presented by the percentage such are NO_x (57%), CO (57%), SO_x (21%) and TSP (16%) by the transport, NO_x (34%), CO (40%), SO_x (37%) and TSP (66%) by the domestic and NO_x (9%), CO (3%), SO_x (42%) and TSP (18%) by industry in and around Kathmandu valley[7]. However, gridded emission inventory of air pollutants eminently exists. Such that the managed and developed of gridded emission inventories is unavoidable for the correct understanding of air pollution on the Kathmandu valley and its surrounding.

2.4 Introduction to key pollutants

2.4.1 Particulate Matter (PM$_{10}$ and PM$_{2.5}$)

Particulate matter is the sum of the all solid and liquid particles suspended in air most of such are hazardous. This complex mixture contains both organic and inorganic particles, which are dust, pollen,

liquid droplets, smoke soot etc. these particle are differ with origin, composition and size. On the basis of their size they are divided in to three main groups: coarse, fine and ultrafine particles. Rough fraction contains the larger particles with a size ranging from 2.5 to 10 micrometer. These particles include dust, pollen and mold spores, fine particles, organic compounds and metals. Ultrafine particles have diameter less than 0.1 micrometer such are also emitted by transportation sector. These particulate matter which area big concern for their health hazard [14]. Exposure to such particles can affect both lungs and heart disease this lead to premature death of human beings and environmental effect are making lakes and stream acidic, changing the nutrient balance in coastal waters and large river basins, reducing visibility, damaging sensitive forests and farm crops, affecting the diversity of ecosystems, contributing to acid rain effect [15]. These type of gaseous to air form transportation system.

2.4.2 Sulfur Dioxide (SO_2)

Sulfur exists in five oxidation conditions in the atmosphere. Sulfur dioxide (SO_2) is the predominant anthropogenic sulfur containing air pollutant. Sulfur dioxide in the atmosphere contributes to secondary aerosol formation through gas- to- particle conversion. The generation of sulfur oxide occurs in the rotary kiln from the oxidization of raw materials. Sulfur Oxides are emitted from sulfur containing fuels in a form of SO_2 and SO_3 when oxidized in the burning zone. According to ENPHO definition, Sulfur dioxide is one of the criteria pollutants that can harm human health and the environment.

2.4.3 Carbon Dioxide (CO_2)

Carbon Dioxide (CO_2) is a naturally occurring gas and a byproduct from the burning of fossil about half of the CO_2 is generated by the combustion of fuel and half from the carbonization of raw materials. The type of fuel used like coal, natural gas, alternate fuel is directly related to the CO_2 emission. These fuels are burned in the kiln during pyro processing.

2.4.4 Carbon Oxide (CO)

The high Coarse of co was found on roadside followed by commercial and residential sectors [16]. CO emitted from indoor activities based on kitchen exposure and also from outdoor activities based on transportation causes various health hazards including respiratory diseases [17, 18].

2.4.5 Nitrogen Oxide (NO_x)

Nitric oxide (NO) and nitrogen dioxide (NO_2), united form known as NO_x are included in the most

important molecules in air pollution. The oxides of Nitrogen are present in the combustion flame from the transport engine [19]. The high temperature range in the kiln acids for the combustion of natural gas with a high flame temperature and results in the generation of significant amount of thermal NO in the kiln.

$N_2 + O \quad \rightarrow \quad NO + N$

$N + O_2 \quad \rightarrow \quad NO + O$
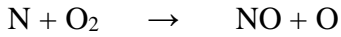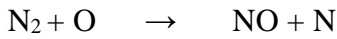
At the exit of the stack under normal atmospheric conditions, the nitrogen oxide is changed to nitrogen dioxide.

$NO + \frac{1}{2} O_2 \rightarrow \quad NO_2$
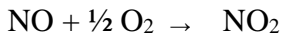
2.5 Meteorological Parameters

The meteorological Parameters associated with the wind play vital role in the prediction of weather conditions and climate process in atmosphere. The weather condition and their implications may be the classified by the demeanor of some key parameters. The some key parameters are discussed in below.

2.5.1 Temperature and Pressure

Pressure decrease exponentially with height from the earth's surface.

$P = P_0 e^{-z/H}$…………………………………………………………………. (2.5)

Here, P = Pressure from the sea level

P_0 = Sea level's Pressure

Z = Height from the sea level

H = Scale height of the atmosphere

The temperature generally decreases with height with lapse rate of ~ 6.5 °C/km whatever, the atmospheric layer is represented by increasing temperature with height called temperature inversion layers. This is also known as stable layer in the atmosphere [19].

2.5.2 Potential Temperature

The temperature of the air parcel when the air parcel is expanded or compressed adiabatically from its existing temperature to standard atmospheric pressure is called Potential temperature. Potential

temperature is represented by θ, which is given as

$$\theta = T \,(P_0/p)^{R/c_p}..(2.5.1)$$

Here,

θ = Potential temperature

T = Instantaneous temperature

P = Instantaneous Pressure

P_0 = Standard pressure

R = Gas constant for 1 kg of air

C_p= Specific heat capacity at constant pressure

The potential temperature (θ) is the preserved quantity for the dry air parcel which moves in the atmosphere adiabatically [19].

The static stability is given by

$$S_z = 1/\theta \,(\partial\theta/\partial z) = 1/T \,(g_0/C_p) + (\partial T/\partial z)............................ (2.5.2)$$

Here,

S_z = Static stability

g_0 = Globally average acceleration due to gravity

z = Vertical height

Equation (2.5.2) gives the following statement for static stability of dry atmosphere.

$(\partial\theta/\partial z) < 0$ Statistically unstable............................ (2.5.3)

$(\partial\theta/\partial z) =$ Statistically stable............................ (2.5.4)

$(\partial\theta/\partial z) >$ Statistically neutral............................ (2.5.5)

2.5.3 Relative Humidity

The ratio of the actual water vapor substance of the air to the maximum amount of the water vapor at the same temperature and pressure is called Relative Humidity. Relative Humidity is with interval 20% - 100% and generally such value reaches maximum before sunrise and minimum at mid-day to late afternoon.

Relative Humidity R_H is given by

$R_H = (w/w_s)\ 100 \approx (\rho/\rho_s)\ 100$ …………………………………… (2.5.6) [19, 20]

Here,

W   = Mixing Ratio with respect to water

Ws = Saturation mixing ratio with respect to water

P   = Vapor pressure

Ps = Saturation Vapor pressure

2.6 Meteorological wind system and flows

The movement of air on different velocity with larger scales is known as wind. Air varies position to position depending upon concern with space scale, speed and element that driven the wind. Mountain regions seen many remarkable weather patterns prevail from differential heating or cooling within mountain slopes. The winds such induced over the mountainous regions are the result of complex topography of mountain and diurnal temperature varies between the winds slopes of the mountainous terrains. There are two kinds of winds seen over the mountainous region, which are named by Terrain forced flow and Diurnal mountain winds.

2.6.1 Terrain forced flow

A flow approaching a mountain barrier will most likely go over the barrier rather than around it if the barrier is long, if the cross- barrier wind component is strong, and if the flow is unstable, near –neutral, or only weakly stable. The degree of stability, speed of flow and terrain characteristics determine the speed and direction of air flow over mountain.
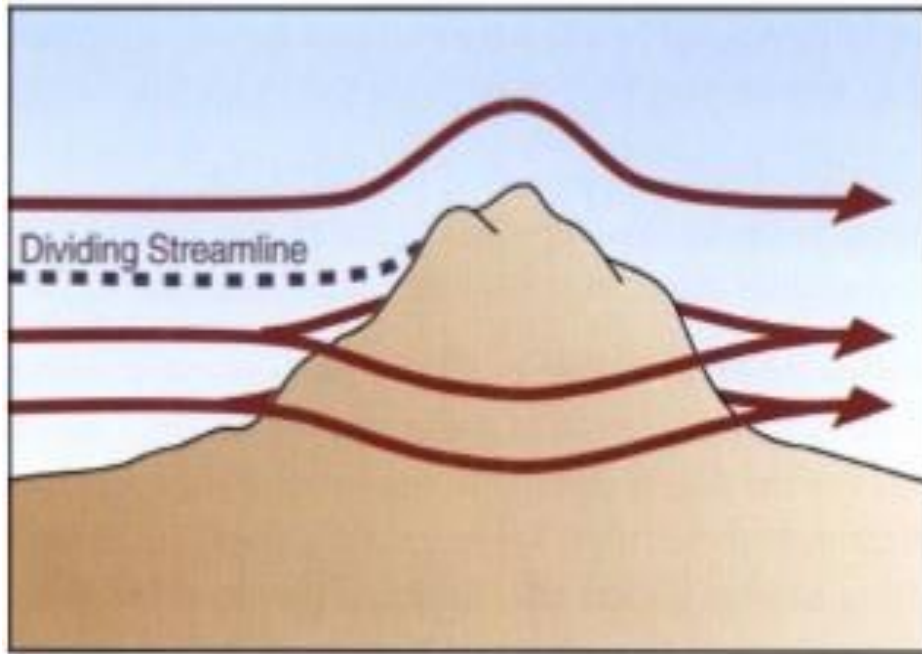
Figure 2.1: Dividing streamline height splits airflow into low- level air and high- level air while approaching to the isolated mountain barrier [21]. Low level air passes around the mountain and converges in leeside and high-level air blow over the mountain barrier.

2.6.2 Diurnal mountain wind

Diurnal mountain winds develop, typically under fair weather conditions, over the slopes of mountainous terrains, from small hills to large mountain massifs, and are characterized by a reversal of wind direction twice per day. Because Diurnal mountain winds are produced by heating of atmospheric layers during daytime and cooling during nighttime, they are also called thermally driven winds. The Diurnal mountain wind system comprises of four system which are slope wind, along valley wind, cross valley wind and mountain plain wind such are depending on the complexities in of terrain [21].
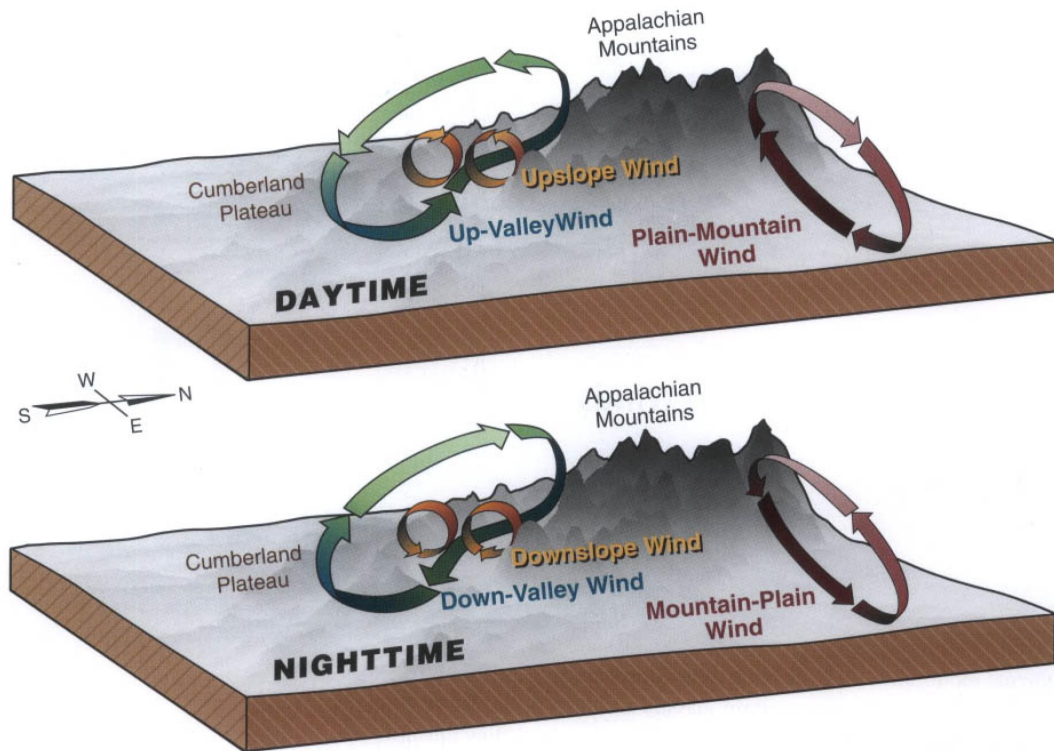
Figure 2.2: Wind systems found over mountainous terrain during daytime and night time [22].

a) The slope wind system

The diurnal thermally driven wind system on the climbs up or drop down direction is called the slope wind system. Two types of slope winds generally prevail over the mountain region. Which are given as

i) The upslope wind

The upslope wind is the local diurnal wind formed, especially on the sloping surfaces. The upslope winds are widespread during daytime. The upslope winds flows are the lower branch of a closed circulation produced by inclined cold boundary layers that form above the slope. Upslope winds are alternatively called an adiabatic winds.
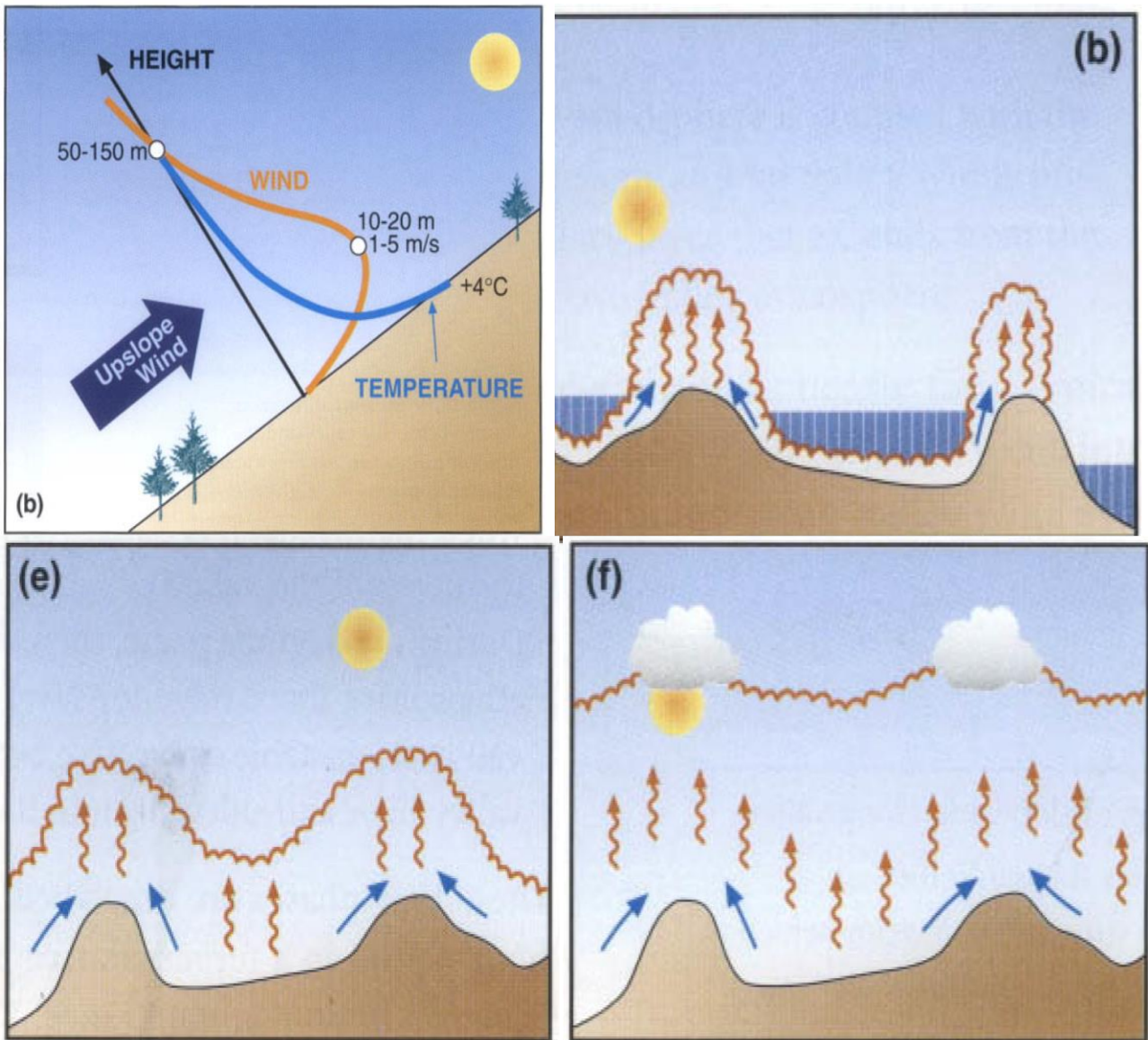
Figure 2.3: The up slope wind system found over mountain terrain during day time

ii) The down slope wind

The down slope wind is also the local diurnal wind formed that blows down the slope of a valley sidewall or an isolated hill or mountain, with down slope flows during night time. The down slope flows are the lower branch of a closed circulation produced by inclined warm boundary layers that from above the slopes. Down slope winds are alternatively called katabatic winds.
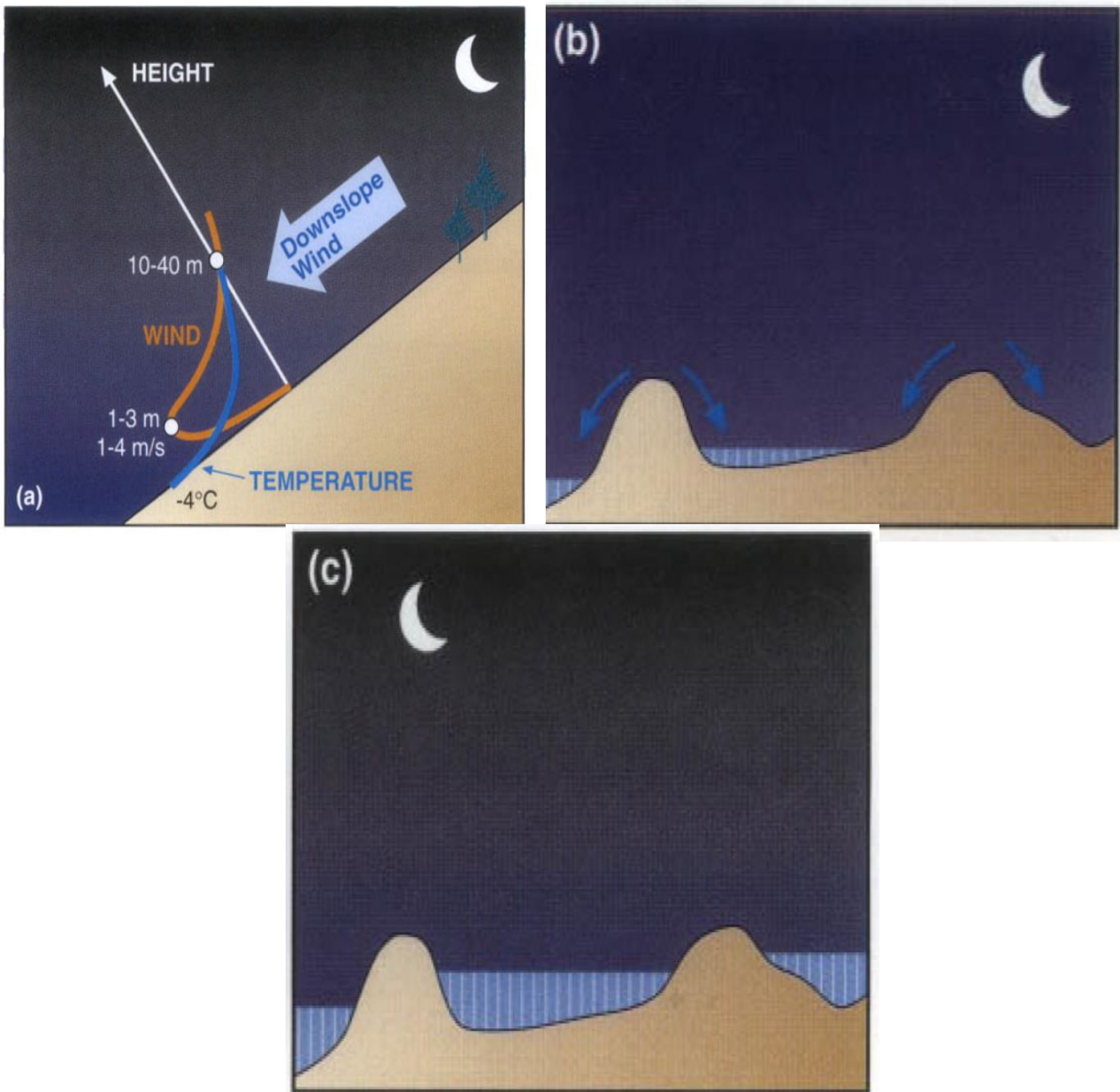
Figure 2.4: The down slope wind system found over mountain terrain during night time.

b) The along- valley wind system

Diurnal valley winds are thermally driven winds that blow along the axis of a valley, with up valley flows during daytime and down-valley flows during night time. Valley winds are the lower branch of a closed circulation that arises when air in a valley is colder or warmer than air that is farther down-valley or over the adjacent plain at the sane altitude.
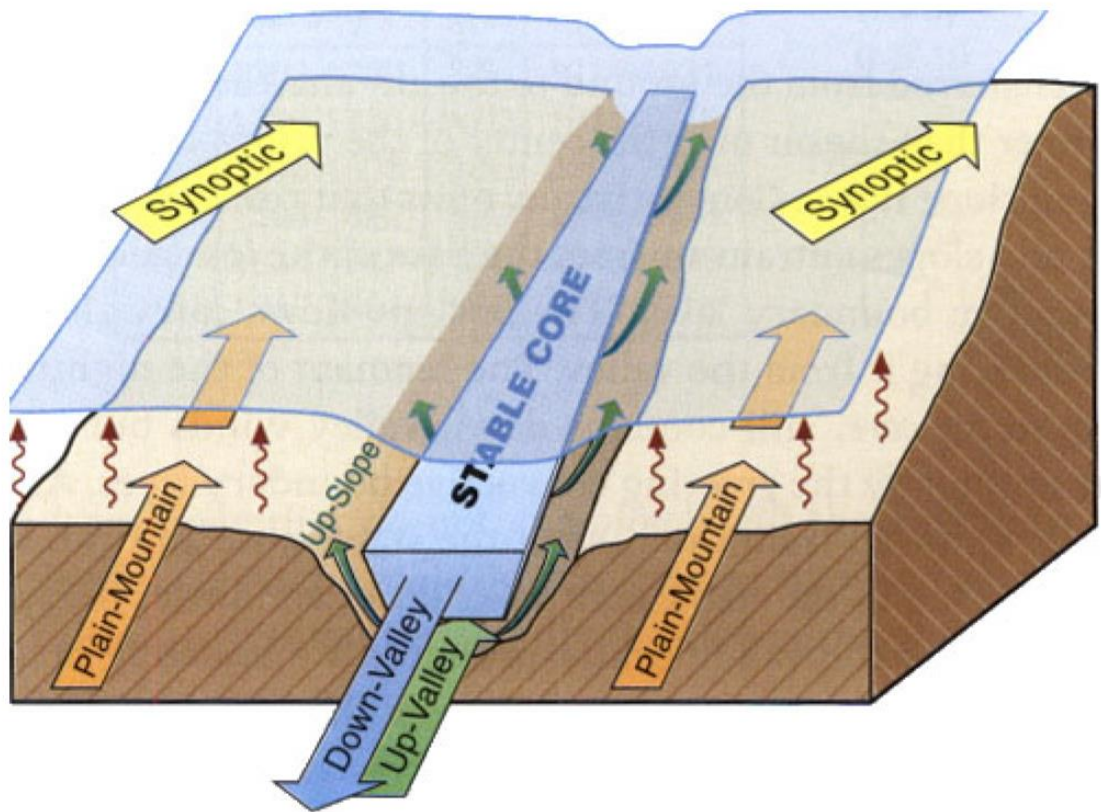
Figure 2.5: The along valley wind system

a) The cross- valley wind system

A wind due to horizontal pressure difference that blows across the longitudinal axis of a valley from one sidewall to another is called cross- valley wind system. This term is usually applied to a thermally driven wind arising when unequal insolation on the two sidewalls causes a strong cross-valley temperature difference. Air then flows toward the more strongly heated sidewall.

b) The mountain- plain wind system

 The day time heating and night time cooling contrast between the mountain atmosphere over the outer slopes of the mountain massif and the free atmosphere over the surrounding plain produces the horizontal pressure differences that drive this wind system, the mountain-plain circulation is associated with a diurnal pressure oscillation between the mountainous region and the adjacent plains. Mountain-plain circulations play a key role in moisture transport and initiation of moist convection also as well as in long-range transport of air pollutants and their precursors.
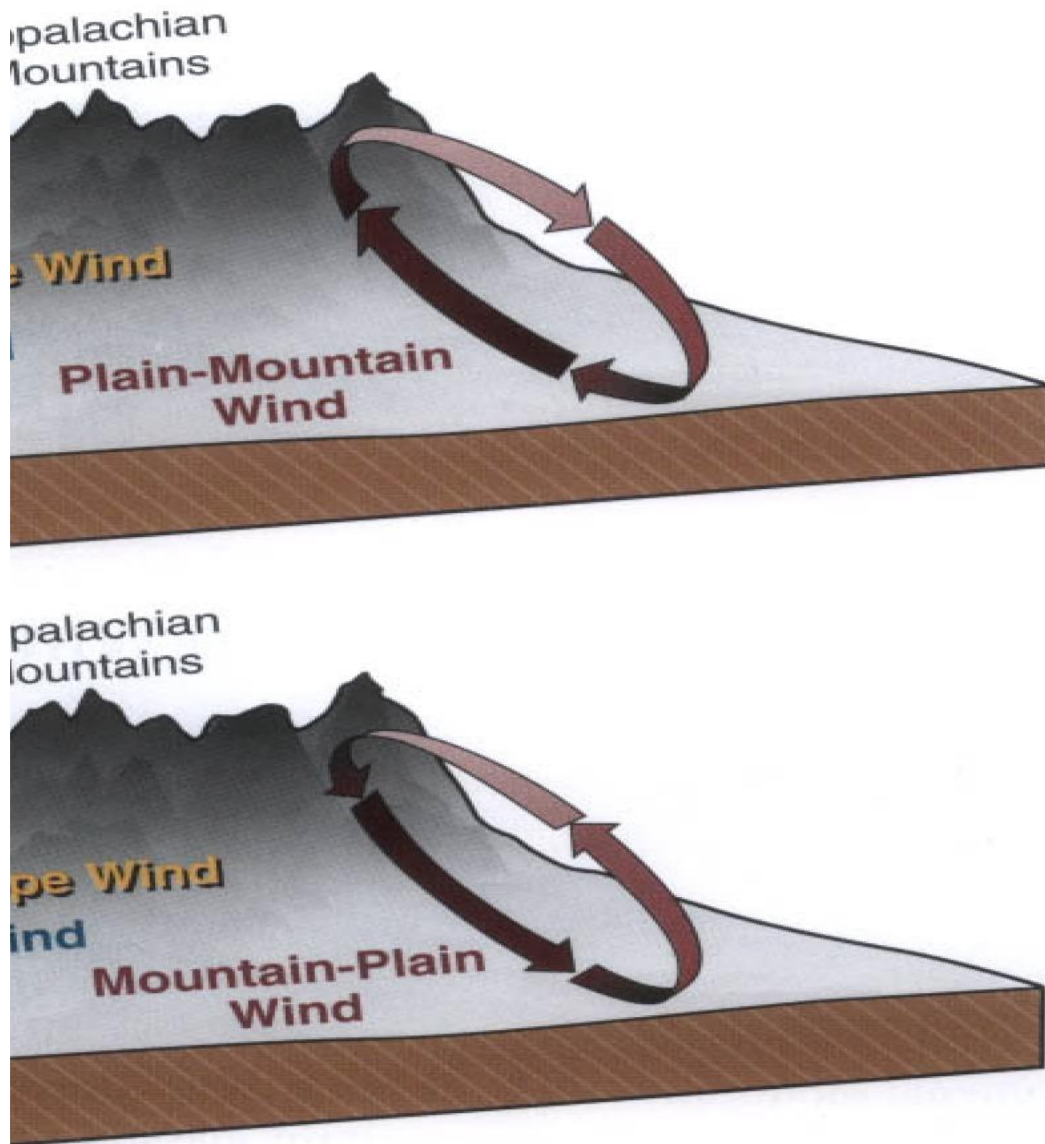
Figure 2.6: The mountain- plain wind system

2.6.3 Atmospheric boundary layer

The lowermost part of the troposphere for which the earth's surface is a boundary on the domain   of the atmosphere is possibly considered as the boundary layer (BL) or often known as atmospheric boundary layer (ABL). Basically, the boundary layer is defined as the compartment of the troposphere that is directly influenced by the presence of the earth's surface (i.e. the lowermost boundary of the atmosphere), and responds to surface forcing with a timescale of about an hour or less. The topmost portion of the air in the atmosphere just above the BL is, termed as free atmosphere (FA) (Fig 2.6.3).

The transport processes like frictional drag, evaporation and transpiration, heat transfer, pollutant emission, and terrain induced flow modification, momentum and heat exchange, etc. at the earth's surface modify the lowest 100 to 3000 m of the atmosphere [23].

The atmospheric boundary layer (ABL) has direct influence on all living species on Earth due to variability of boundary surface characteristics (shape, roughness, albedo, moisture content, heat emissivity), and heat capacity determine the momentum and energy exchange between the surface and the atmosphere. This layer bonds the Earth's atmosphere to the remaining sections of the Earth system [23, 24]. Thus, ABL research assists in creation of part of atmospheric sciences and meteorology, and has become an essential part of researches like Earth system research and Global Change research as well.
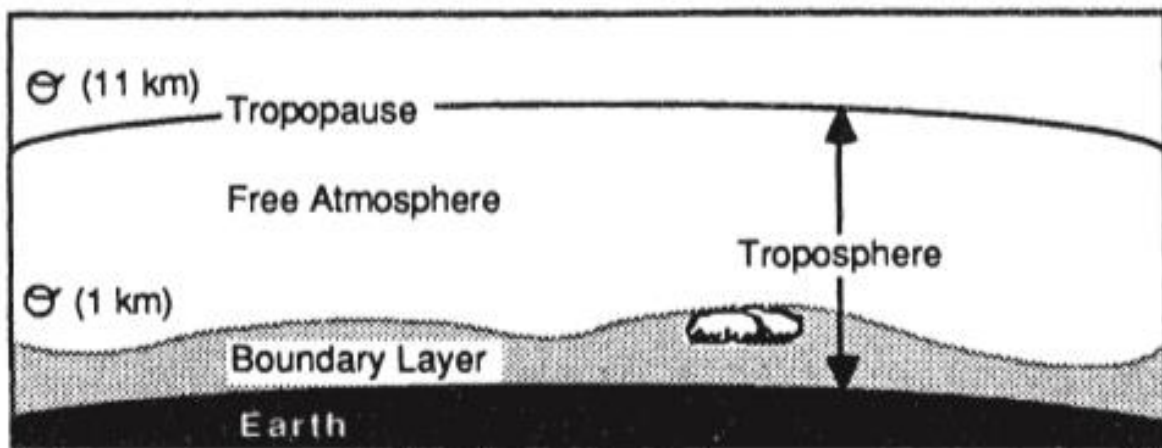
Figure 2.7: The troposphere can be divided into two parts: a boundary layer (shaded) near the earth's surface and the free atmosphere above it [25].

a) Boundary Layer Height (BLH)

The overall thickness of the ABL is identified as the boundary layer height (BLH) or BL depth. The lowest bottom of the ABL is termed as the surface layer (SL) which is 10% of the total ABL depth. With the largest velocity gradients, the planetary boundary layer turbulence is produced in this SL, i.e. due to aerodynamic drag, there is a wind gradient in the wind flow just a few hundred meters above the Earth's surface.

Over oceans, the BL depth variations result relatively slowly in space and time out of which most of the variations in BL depth over oceans are due to synoptic and mesoscale processes of vertical motion and advection of different air masses over the sea surface.

Generally, over both land and oceans, the BL is slender of nature in high-pressure regions than in low-pressure regions (Fig 2.7). The subsidence and low-level horizontal divergence associated with synoptic high pressure moves boundary layer air (BLA) out of the high towards lower pressure regions. The shallower depths are often associated with cloud-free regions. If clouds are present, they are often fair-weather cumulus or stratocumulus clouds.

In low pressure regions the upward motions carry BLA away from the ground to large altitudes throughout the troposphere. It is difficult to define a boundary layer top for these situations. Cloud base is often used as an arbitrary cut-off for boundary layer studies in these cases. Thus, the region studied by boundary layer meteorologists may actually be thinner in low-pressure regions than in high pressure ones (Fig 2.8).
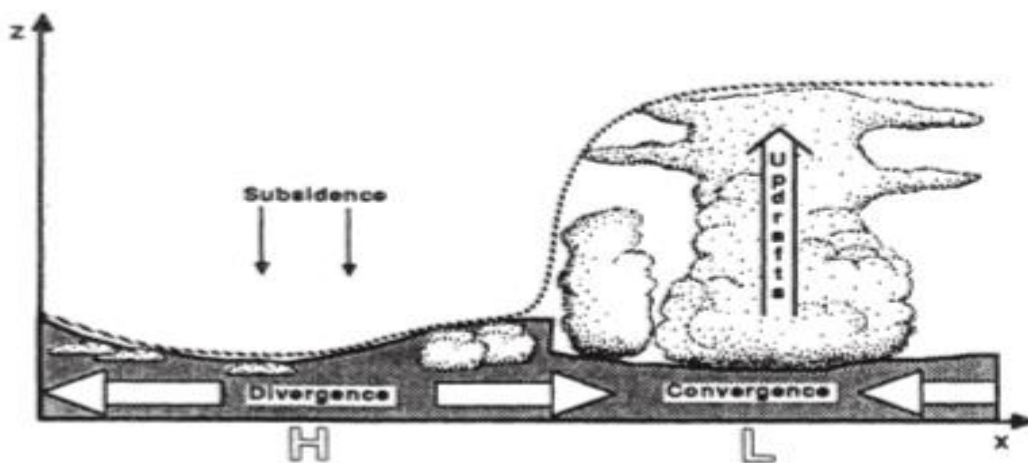
Figure 2.8: Schematic of synoptic -scale variation of boundary layer depth between centres of surface high (H) and low (L) pressure [24].

Over land surfaces in high pressure regions the BL has a well-defined structure that evolves with the diurnal cycle (Fig 2.6.3 b). The three major components of this structure are the mixed layer (ML), the residual layer (RL), and the stable boundary layer (SBL). When clouds are present in the mixed layer, it is further subdivided into a cloud layer (CL) and a sub cloud layer

23

a) Convective Boundary Layer

Convection is the scientific name for thermal. The convective boundary layer, hereinafter referred as CBL, sometimes called the atmospheric mixing layer or dry adiabatic layer is the lower tropospheric layer in contact with the ground heated by the sun and swept by the wind (s_1, s_6 in Fig 2.6.3 b). It is so called the convective mixed layer because there is a significant air mixing with horizontal and vertical turbulences by dynamic one (wind) throughout the phenomenon of convection. In other words, it is the layer mixed by dry thermals or (vertical) wind shear [26].

In the absence of complete cloud cover, the convective boundary layer (CBL) over land shows a strong diurnal development, and in mid-latitudes in summertime typically reaches a height of 1-2 km by mid-afternoon. From sunrise on, and throughout the daylight hours, this development (Fig 2.6.3 b) includes the following:

a) The breakdown of the nocturnal inversion through heating, and the development of a shallow, well-mixed layer (s_1 and s_6 in Fig 2.6.3 b)
b) Prior to sunset, development of a surface inversion related to surface cooling (s_2 in Fig 2.6.3 b).

Thus, surface cooling due to heat flux emission from earth after sunset and before next sunrise results the convective mixed layer dilution just over the nocturnal boundary layer height and this diluted convective mixed layer is termed as Residual Layer (s_2 and s_3 in fig 2.6.3 b) [27].
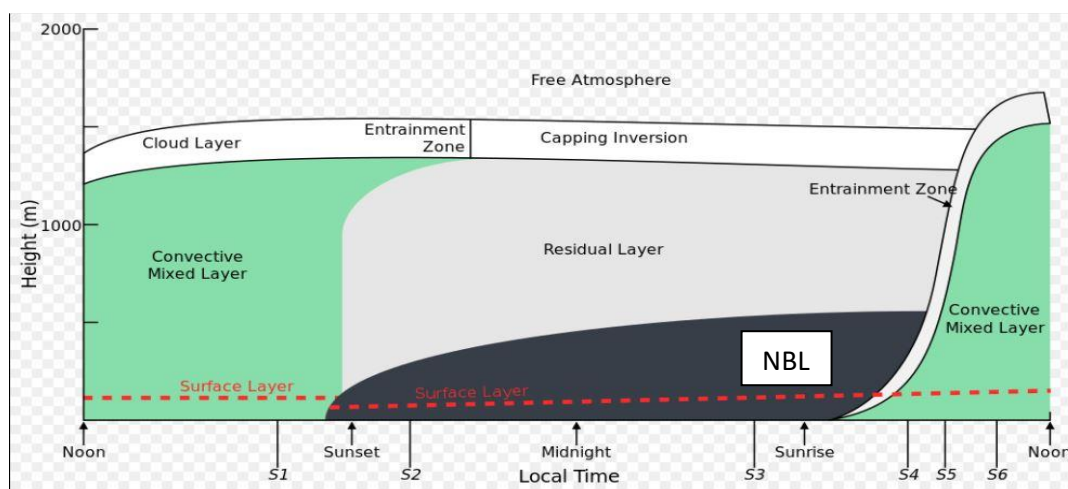

Figure 2.9: A diagram of the ABL in high pressure regions over land consists of three major parts: At sunrise, heating from below sets to a convective boundary layer (CBL), while at sunset heat loss to space terminates convection and creates a thin nocturnal boundary layer (NBL) [24]

24

b) Stable Boundary Layer

The ABL is called as stable boundary layer (SBL) if the earth's surface is cooler than the air when negative buoyancy flux at the surface damps the turbulence. Particularly, wind shear turbulence helps to drive the SBL solely therefore it is difficult to recognize the existence of SBL without the free atmosphere wind. An SBL becomes specific in the land where the surface is colder than the air over that land at day time as well as night time. At night, over this land the SBL is defined as the nocturnal boundary layer (NBL). The process of advection of warmer air over the cooler air intensify the formation of NBL.

In high latitudes of very cold temperatures, the SBL predominantly plays an important role in which it remains longer than (day to months). Due to the coldness, the mixing process is very low because of which even less pollution is very harmful.

Always the existence of SBL turbulence is not found to be homogeneous according as the place. Sometimes it becomes sporadic and patchy which disengage the upper portions of the ABL from surface forcing.

These considerable variation of ABL overall in depth may occurs from a few tens of metres to several kilometres. Thus, in any case, only the detection of state of the surface layer that creates the lowest part of the ABL, is being capable by the surface observations and measurements [23, 24].

c) Mixing Layer Height (MLH)

The mixing layer height (MLH) within the ABL may be identified as the height up to which the uniform dispersion of atmospheric properties like wind speed and turbulence or other matters that originated from the earth's surface is generated due to active turbulent vertical mixing processes. For the identification of ML and MLH, other kinds of atmospheric parameters such as potential temperature, specific humidity or aerosol particle concentrations behave as favourable conservative variables. Despite of the MLH is shallower than the ABL, it can cover the entire ABL in intensive CBLs since the ML (if it exists) is a part of the ABL [24]. In day-time generally, we use the name MLH, is about identical to BLH (generally named at night) in clear skies because of happening large mixing processes during day time however the low mixing forms the SBL at night time.

MLH is an important parameter of ABL that enhances to understand the atmospheric transport processes like air pollution, weather and climate change in the troposphere [28].

The Public transport is related with transportation of local passengers so PT is also increasing and developing with increasing passengers in urban area like a Kathmandu Valley, Due to this reason air pollution is also increasing in urban city Therefore, PT study is very important to recognize about specific and adverse impacts that fall into human health as well as the other living creatures due to anarchy in emission characteristics by the diurnal pollution activities on the surface, Changes to the ground shield, climatological and meteorological variations, atmospheric chemical change, temperature variation in water and landing areas.

Chapter 3

METHODOLOGY

3.1 Introduction

This chapter discusses the methodological and the procedural approaches adopted in achieving the objective of the study. The methods and procedures implemented in the study may be conceptualized as in the chart below.
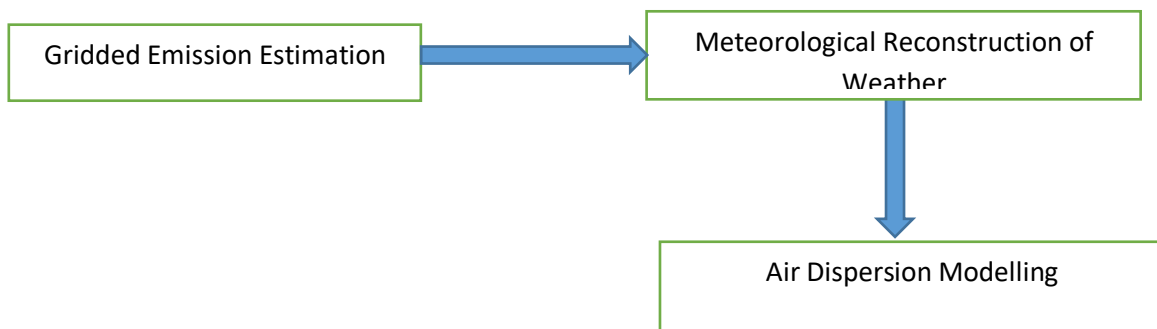

Figure 3.1: Conceptualized frame work of research methods and procedures adopted.

It has been mentioned the detail methodology in figure 3.2 to achieve the overall objectives of research. The NCEP meteorological data and USGS land use data use as an input data on the WRF model give the meteorological data for the research area and will be validated by surface or field observation. The WRF model is used for the weather simulation. When the model is validated, then the different sources of pollutant from private vehicle have been spatially localized in their position using ArcGIS 10.6. Finally, CTM simulations give rise to the dispersion map of major pollutants and displays these on area map with 1 km $\times$ 1 km horizontal grid resolution. Each component of the method of study are discussed in the following sub-sections.
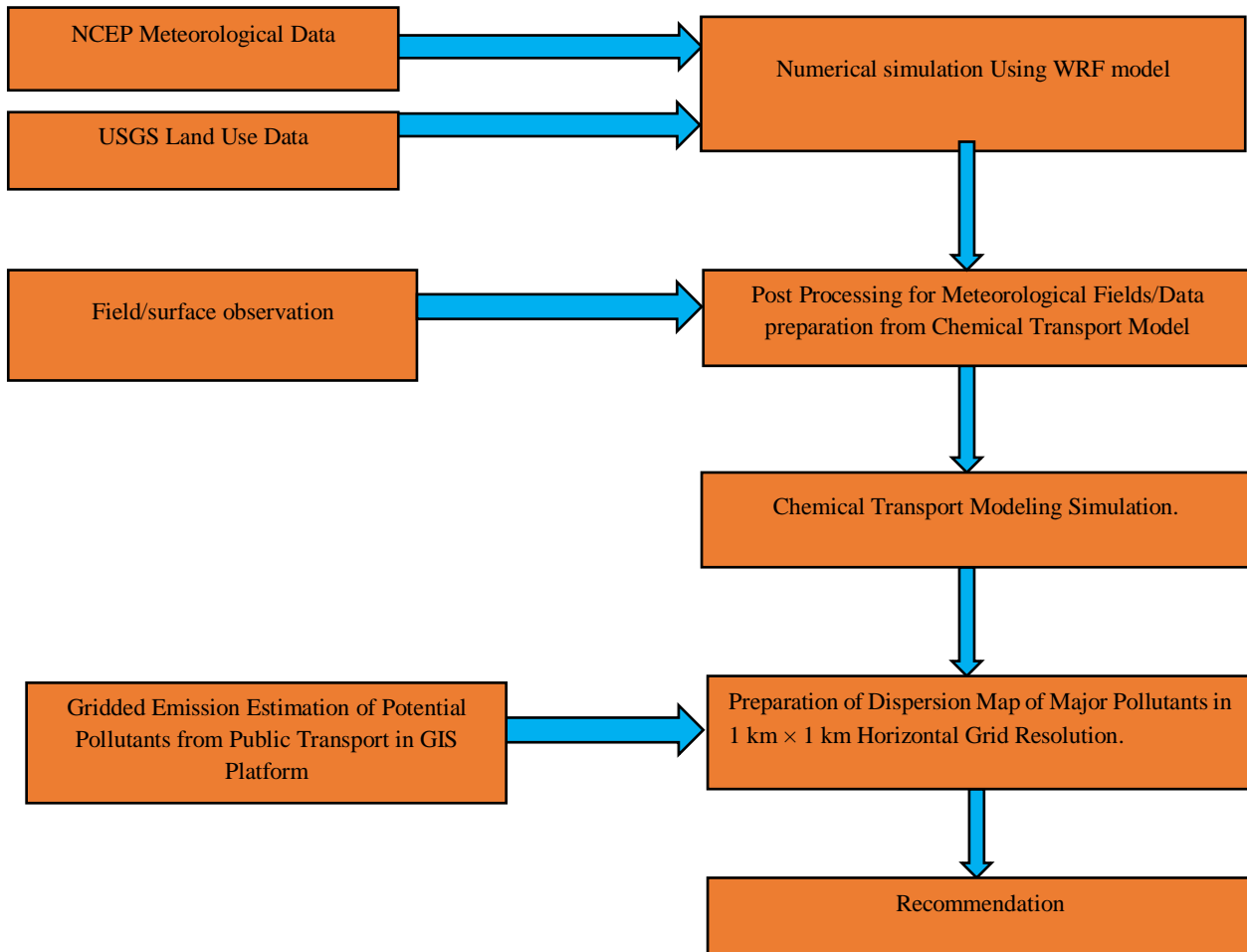
Figure 3.2: Flow chart showing methodology for air pollution dispersion modelling.

3.2 Gridded Emission Inventory

The gridded emission estimation provides us the details of the spatial distribution of pollutant sources and magnitude of emission over the area of interest. A dependable gridded map and emission inventories of pollutants is considered to be the perquisite to initialize chemical transport modelling and hence to prepare air pollution air shed map. The air pollution air shed map enables us to determine the spatial and temporal distribution of pollutants blanketing the area of interest and hence to evaluate exposure people vegetation and properties of pollutants. The schematic demonstration of method applied for preparing gridded emission inventory from different sectors is depicted in the Figure 3.3.
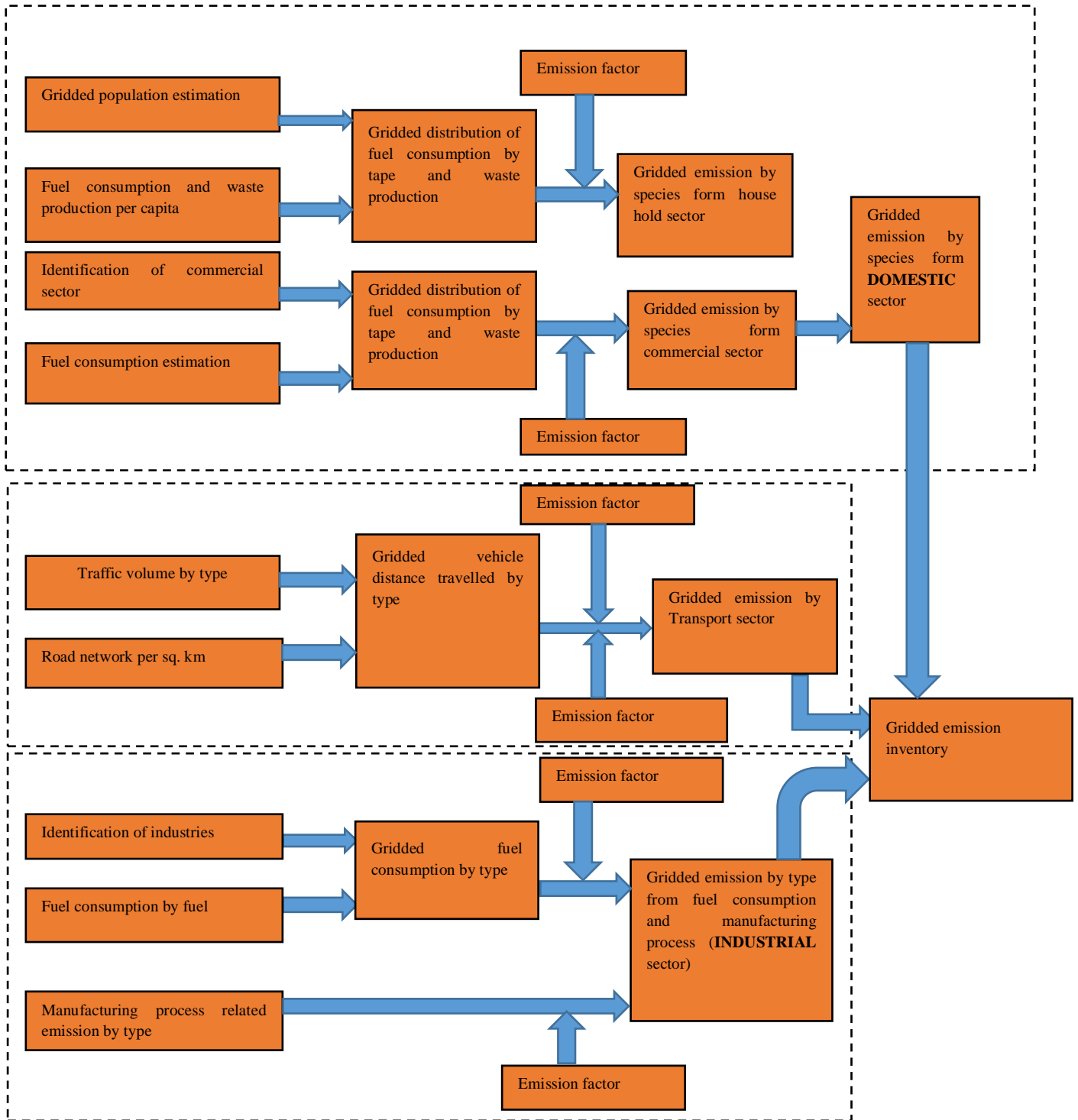
Fig 3.3: Schematic demonstration of method applied for preparing gridded emission inventory from different sector [29].

Figure 3.4: Google Earth view of the Kathmandu valley (red circled area) over which gridded emission inventories were prepared for Public Transport.

Present study has developed gridded emission map for major pollutants (TSP, SO$_2$, NOx and CO) for the public transport fleet of Kathmandu valley as per the schemes outlined in the Figure 3.3. Sources of the potential pollutants have been spatially localized in their position using ArcGIS 10.6. The inventories are prepared for the area of 70 km x 70 km are surrounding the Kathmandu valley using the ArcGIS 10.6 with a horizontal grid resolution of 1km $\times$ 1km. The centre of the emission estimation domain was placed at the centre of the valley (27.7° N, 85.3° E). Figure 3.4 shows the Google Earth view of Kathmandu valley over which gridded emission inventories were prepared for public Transport fleet. Emission of pollutant species has been calculated in each grid using the emission factors as described in the Atmospheric Brown Cloud (ABC) Emission Inventory Manual, 2013 [29].

The estimation used the following formulation for the public Transport fleet:

a) $\sum_{\text{Public transport}}$ (number of taxies) $\times$ (grid public vehicle kilometer travelled) $\times$ (emission factor per kilometer travel)

The pollutants released by Public Transport fleet includes CO, CO2, SO2, NOX, $PM_{2.5}$, PM_{10}, TSP, NMVOC etc. Among these pollutants, present study is specially focused on the emission and dispersion of the particulate pollutant $PM_{2.5}$.

3.3 Meteorological Simulation

The prevailing meteorological fields over the Kathmandu valley during the winter season was numerically simulated using the Weather Research and Forecasting (WRF) modelling system. Following several sub-sections introduces the different component of the WRF model [30].

3.3.1 The WRF Model

The atmospheric phenomena, non-linear in characteristics, should naturally be governed by non-linear equations. Various numerical atmospheric model have been developed and are used widely. However, not all the models performs well for all the atmospheric and topographic situations. Present study uses the WRF model as it has been reported to perform well in the complex terrain of Nepal Himalaya. [31, 32].It attributes two dynamical cores, a data adjustment system, and a software framework smoothing parallel computation and system flexibility. The two dynamical cores are the Advanced Research WRF (ARW) and Non-hydrostatic Mesoscale Model (NMM). Dynamical core incorporates generally Coriolis, pressure gradients, buoyancy, filters, diffusion, advection and time stepping. WRF is suitable for large eddy to global scale simulations and include real-time NWP data assimilation development and studies, parameterized-physics research, regional climate simulations, air quality modelling, atmosphere-ocean coupling and idealized simulations. Apart from this, WRF is an innovative, effective and successful model for the study of weather phenomena, atmospheric dynamics, atmospheric boundary layer and cloud microphysics [33, 34]. The overview of WRF modelling is represented in Figure 3.5.

Components of WRF Model

The WRF modelling consists of these major programs:

- The WRF processing system(WPS)

- WRF_Var

ARW solver Post processing and visualization tools

A) The WPS

The WPS processing system (WPS) is set of three program whose collective role is to prepare input to the real program for real data simulation. Its functions include

1. Defining simulation domains

2. Interpolating terrestrial data (such as terrain, land use and soil types) to the simulation domain.

3. Degribbing and interposing meteorological data from another model to this simulation domain.

Following utilities are exploited in WPS for the preparation on inputs for the dynamics core of the model.
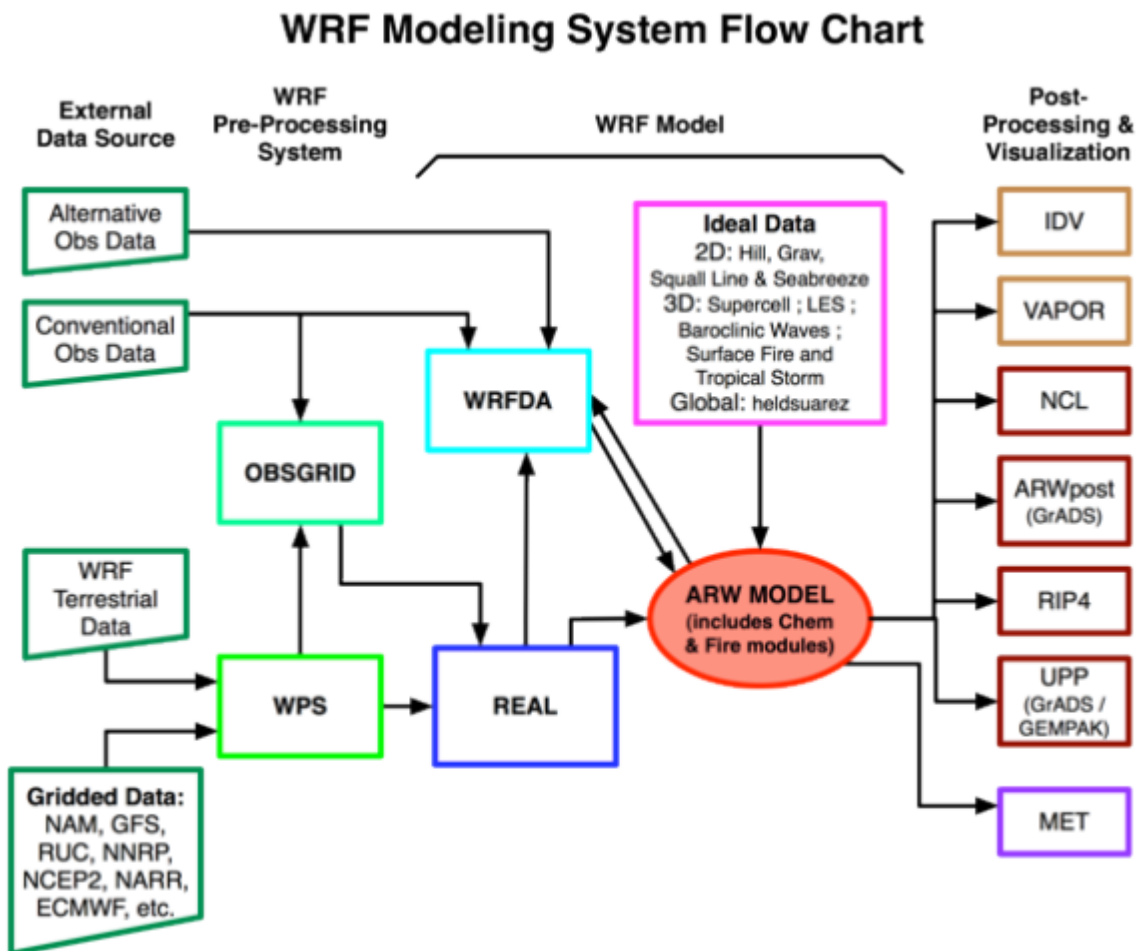

Figure 3.5: WRF flow chart [35]

a) The Geogrid

Defines simulation domain and ARW nested domains. It interpolates the static geographic data to the grids of the model domain. In addition to computing the latitude, longitude and map scale factor at every grid point, geogrid will interpolate soil categories, land use category, terrain height, annual mean deep soil temperature, monthly vegetation fraction, monthly surface albedo, maximum snow albedo, and slope category to the model grids by default. The simulation domains are defined using information specified by the user in the geogrid name list record of the WPS name list file, name list. Wps.Global data sets for each of these fields are provided through the WRF download page. New or additional data sets may be interpolated to the simulation domain through the use of the table file, GEOGRID.TBL. The GEOGRID.TBL file defines each of the fields that will be produced by geogrid; it describes the interpolation methods to be used fora field, as well as the location on the file system where the data sets for that field is located.

b) The Ungrib

It degribs or extracts the Grib format meteorological fields into intermediate format. GRIB files typically contain more fields than are needed to initialize WRF. The GRIBfiles contain time-varying meteorological fields and are typically from another regional or global model, such as NCEPs NAM or GFS models. Ungrib uses tables of these codes-called V tables, for variable tables to define which fields to extract from the GRIB file and write to the intermediate format. Ungrib can write intermediate data files in anyone of three user-selectable formats: WPS, SI and MM5 format. Any of these formats may be used to initialize WRF.

c) The Metgrid

The metgrid program horizontally interpolates the intermediate-format meteorological data that are extracted by the ungrib program onto the simulation domains defined by the geogrid program. The interpolated metgrid output can then be ingested by the WRF real program. The range of dates that will be interpolated by metgrid are defined in the "share" name list record of the WPS name list file, and date ranges must be specified individually in the name list for each simulation domain. Since the work of the metgrid program, like that of the ungrib program, is time-dependent, metgrib is run every time a new simulation is initialized. Control over how each meteorological filed is interpolated is provided by the METGRID.TBL. The METGRID.TBL file provides one section for each field, and within a section, it is possible to specify options such as the interpolation methods to be used for the field. Output from metgrid is written in the WRF I/O API format, and thus, by selecting the Net CDF

I/O format, metgrid can be made to write its output in NetCDF for easy visualization using software packages, including RIP4.

B) ARW Solver

This is the key component of the modelling system, which is composed of several initialization programs for idealized, and real-data simulations, and the numerical integration program.

C) Post Processing and Visualization Tools

Several programs are supported, including RIP4 (Read, Interpolate and Plot) (based on NCAR Graphics), NCAR Graphics Command Language (NCL), and conversion programs for other readily available graphics like GrADS.

3.3.2 Governing Equations of WRF model

The ARW dynamics solver integrates the compressible, non-hydrostatic Euler equations. The ARW equations are expressed by using terrain following hydrostatic pressure vertical coordinate denoted by η based on [36] and are defined as

$$\eta = \frac{(P_h - P_{ht})}{\mu} \tag{3.7}$$

Where, $\mu = (P_{hs} - P_{ht})$, P_h is the hydrostatics components of the pressure, P_{hs} and P_{ht} refers values along the surface and top boundaries, respectively (see Figure 3.8). The value of η varies from 1 at the surface to 0 at the upper boundary of the model, domain.
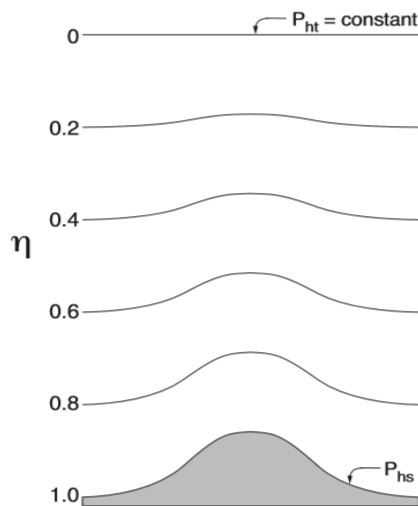

Figure 3.6: Terrain following vertical pressure coordinate system (η) used in WRF ARW modelling system [36, 37].

This vertical coordinate is also called a mass vertical coordinate. Since μ (x, y) represents the mass per unit area within the column in the model domain at (x, y), the appropriate flux form variables are,

$$\mathbf{V} = \mathbf{\mu v} = (U, V, W), \Omega = \mu\dot{\eta}, \Theta = \mu\theta. \qquad (3.8)$$

Where, $\mathbf{v} = (u, v, w)$ are the covariant velocities in the two horizontal and vertical directions, respectively, while $\omega = \dot{\eta}$ is the contravariant 'vertical' velocity. θ is the potential temperature. Also appearing in the governing equations of the ARW are the non-conserved variables $\Phi = gz$ (geopotential), p (pressure), and $\alpha = \frac{1}{\rho}$ (the inverse density of air).

The Flux-form Euler equation [61] which are the governing equation for WRF model are,

$$\partial_t U + (\nabla.\mathbf{V}u) - \partial_x(p\phi_\eta) + \partial_\eta(p\phi_x) = F_U \qquad (3.9)$$

$$\partial_t V + (\nabla.\mathbf{V}v) - \partial_y(p\phi_\eta) + \partial_\eta(p\phi_y) = F_V \qquad (3.10)$$

$$\partial_t W + (\nabla.\mathbf{V}w) - g(\partial_\eta p - \mu) = F_W \qquad (3.11)$$

$$\partial_t \Theta + (\nabla.\mathbf{V}\theta) = F_\theta \qquad (3.12)$$

$$\partial_t \mu + (\nabla.\mathbf{V}) = 0 \qquad (3.13)$$

$$\partial_t \Theta + \mu^{-1}[(V.\nabla\phi - gW)] = 0 \qquad (3.14)$$

$$\partial_\eta \phi = -\alpha\mu \qquad (3.15)$$

And the equation of state is given by,

$$p = p_0 \left(\frac{R_d\theta}{p_0\alpha}\right)^\gamma \qquad (3.16)$$

Where α represents a generic variable. $\gamma = \frac{C_p}{C_v} = 1.4$ is the ratio of specific heat capacities for dry air, R_d is the gas constant for dry air and p_0 is a reference pressure (typically 10^5 pascals).

Here, the subscripts x, y and η denote differentiation,

$$\nabla.Va = \partial_x(U_a) + \partial_y(V_a) + \partial_\eta(\Omega_a) \qquad (3.17)$$

$$\nabla.\nabla a = U\,\partial_x a + V\,\partial_y a + \Omega\,\partial_\eta \qquad (3.18)$$

Other variables are:

V: three-dimensional coupled vector velocities

P: pressure

μ: pressure difference between surface and top of the model

ɸ : Geopotential

Θ : Coupled potential temperature

g: acceleration due to gravity

U: coupled horizontal component of velocity in the x-direction

V: coupled horizontal component of velocity in the y-direction

W: coupled horizontal component of velocity in the z-direction

U: horizontal component on velocity in x-direction

V: vertical component of velocity

Here, equations (3.9) and (3.10) are the horizontal momentum equations whereas equation (3.11) is the vertical momentum equation. Equation (3.12) is the conservative potential temperature equation. Equation (3.13) is the conservative equation for dry air. Similarly, equation (3.14) determines the geopotential and is only the equation which is non-conservative equation. Equation (3.15) governs inverse density equation and equation (3.16) is the equation of state. The WRF model assigns the use of four projections: the Lambert conformal polar stereographic, Mercator, and Latitude-Longitude. Each grid point inside the WRF model has the same horizontal dimension. However, the grid points are then projected onto the Earth and are allowed to have slightly different sizes, to fit properly to the map projection. This is achieved by using map scale factors, which require the governing equations from (3.9) – (3.16), and momentum variables, to be redefined [37]. The governing equations are further written using perturbation forms to reduce truncation errors in the horizontal pressure calculation, as well as buoyancy calculation. The new variables are perturbations from a hydrostatically balanced reference state. This causes changes to the momentum equations, the equation for mass conservation and the geopotential equation [37]. These equations, as well as the equation of state, are solved by the WRF model, and contain a Coriolis term, mixing term, as well as parameterized physics.

3.3.3 Model setup and Initialization

The WRF modelling system was initialized with the meteorological data from National Centre for Environmental Prediction (NCEP) with resolution of $1° \times 1°$ over Kathmandu valley has been performed. The domain system consists of triply nested two-way interacting mesh. Both coarse (D1) and fine (D2) domain consists of $52 \times 52 \times 35$ grid points with horizontal grid size of 9 km and 3 km respectively, whereas the finest domain (D3) include $70 \times 70 \times 35$ grid points with horizontal grid size of 1km as depicted below (see Figure 3.9). All three domains are placed at (27.7° North and 85.3° East) center of Kathmandu valley in the western central area. Three days NCEP Meteorological data starting from 7th to 9th December, 2018 has been simulated. The first day of the simulation was discarded as a spin-up period of the model and the remaining two days has been expended for the analysis. Moreover, the model used 24-category land-use and 30-second terrain elevation data of the United States Geological Survey (USGS). Its hourly outcomes are used as meteorological parameters for the Chemical Transport Model (CTM).
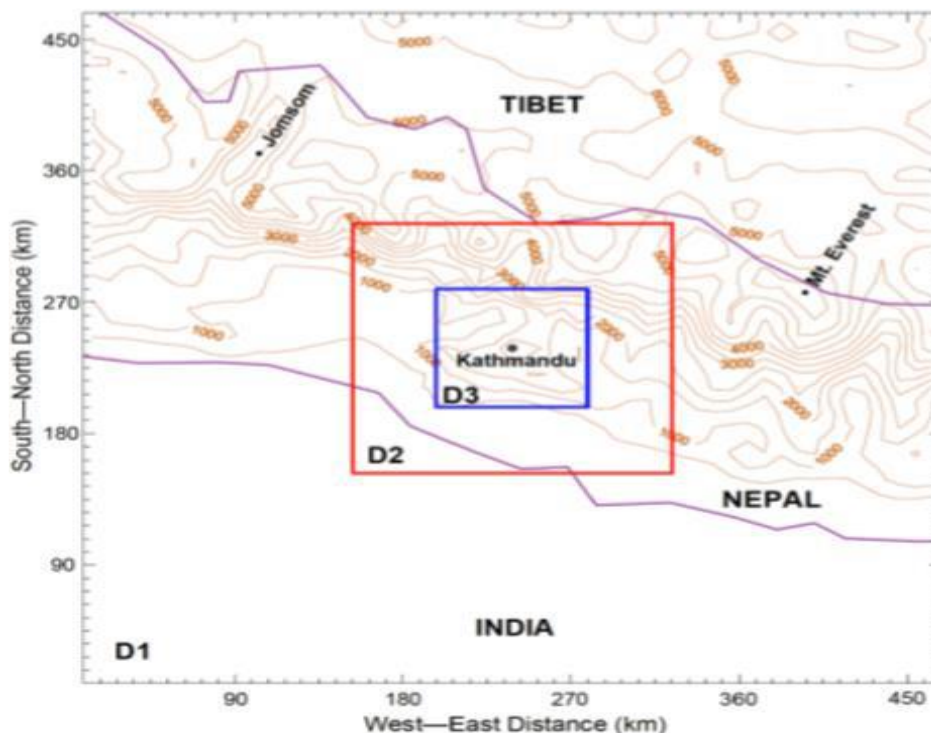
Figure 3.7: triply nested two-way interacting calculation domain configuration used in the study of meteorological flow system centred at 27.7° N, 85.3° E for the Kathmandu valley.

The inner most domain box shows the area over which meteorology and air pollution transports are discussed. The physics scheme adopted in this calculation include Dudhia scheme [38] for shortwave radiation, Rapid Radiative Transfer Model (RRTM) scheme [39] for long-wave radiation, the

Thompson graupel scheme [40] for cloud microphysics, MYJ scheme [41] for planetary boundary layer, and the Noah land-surface model [38] for calculations with the WRF.

3.4 Air Pollution Dispersing Modelling

3.4.1 Chemical Transport Model (CTM)

An atmospheric dispersing model can numerically simulates/predicts the dynamics pollutants released over the study area. Like in the case of meteorological models, number of chemical transport model (CTM) are available each having different strengths and weaknesses.

However, present study used the CTM which has been reported to perform well for air pollution dispersion modeling over the complex terrain of the Kathmandu valley [42, 43, and 44]. It deals with the 58 chemical species and include a system of 130 chemical reactions.

3.4.2 Advection equation of CTM model

The main part of Chemical Transport Model (CTM) model is based on [44]. This model uses a terrain following vertical coordinate. The Equations 3.23-26 represent the basic equations used in the model.

$$
\begin{aligned}
\frac{\partial \Delta H \sigma X_i}{\partial \tau} &+ \frac{\partial \Delta H \sigma_u X_i}{\partial \xi} + \frac{\partial \Delta H \sigma_v X_i}{\partial \eta} + \frac{\partial \Delta H \sigma_w X_i}{\partial \tau} \\
&= \frac{\partial}{\partial \xi}\left\{\Delta H \sigma K_H\left[\frac{\partial X_i}{\partial \xi} - \frac{1}{\Delta H}\frac{\partial X_i}{\partial \rho}\left(\frac{\partial h}{\partial \xi} + \rho\frac{\partial \Delta H}{\partial \xi}\right)\right]\right\} \\
&+ \frac{\partial}{\partial \eta}\left\{\Delta H \sigma K_H\left[\frac{\partial X_i}{\partial \eta} - \frac{1}{\Delta H}\frac{\partial X_i}{\partial \rho}\left(\frac{\partial h}{\partial \eta} + \rho\frac{\partial \Delta H}{\partial \eta}\right)\right]\right\} \\
&+ \frac{\partial}{\partial \rho}\left\{\frac{\sigma}{\Delta H}\left[K_v + K_H\left(\frac{\partial h}{\partial \xi} + \rho\frac{\partial \Delta H}{\partial \xi}\right)^2 + K_H\left(\frac{\partial h}{\partial \eta} + \rho\frac{\partial \Delta H}{\partial \eta}\right)^2\right]\frac{\partial X_i}{\partial \rho}\right. \\
&\left. - \sigma K_H\left(\frac{\partial h}{\partial \xi} + \rho\frac{\partial \Delta H}{\partial \xi}\right)\frac{\partial X_i}{\partial \xi} - \sigma K_H\left(\frac{\partial h}{\partial \eta} + \rho\frac{\partial \Delta H}{\partial \eta}\right)\frac{\partial X_i}{\partial \eta}\right\} + \Delta H \sigma R_i + \Delta H \sigma S_i
\end{aligned}
$$

Where,

X_i is dimensionless concentration of ith species.

σ is air density, R_i and S_i are the chemical reaction rate and source strength of ith species.

As,

$\xi = x, \eta = y, \tau = t$ and

$$\rho = \frac{z-h(x,y)}{H(x,y,t)-h(x,y)} = \frac{z-h(x,y)}{\Delta H(x,y,t)} \tag{3.24}$$

Where $h(x, y)$ and $H(x, y, t)$ represent terrain height and height of upper boundary above the mean sea level respectively and $\Delta H(x, y, t) = H(x, y, t) - h(x, y)$

ρ Varies from 0 at bottom surface to 1 at upper boundary surface above the mean sea level and W represents the vertical velocity and in η, ξ and ρ coordinates.

$$W = \frac{1}{\Delta H}\left[w - u\left(\frac{\partial h}{\partial \xi} + \rho\frac{\partial \Delta H}{\partial \xi}\right) - v\left(\frac{\partial h}{\partial \eta} + \rho\frac{\partial \Delta H}{\partial \eta}\right) - \rho\frac{\partial \Delta H}{\partial \tau}\right] \tag{3.25}$$

Where, u, v and w are velocity component of wind x, y, z direction respectively.

For redial species, a steady state assumption has been implied and it gives

$$R_i = 0, i = n + 1, \ldots \ldots, i \tag{3.26}$$

For the solutions of equations (3.23) and (3.24), the finite element method for transport equations and semi analytical methods for chemistry has used after separating equations (3.23) has been separated into its transport and chemical parts [44, 45, 46]. Time steps for numerical integration are 5 minutes for transport and 12 seconds for chemistry.

3.4.3 Modelling domain system

The center of the domain was set Kathmandu valley with latitude 27.7° N and longitude 85.3° E. The calculation domain of area 70 km × 70km was used for the calculation of dynamics of pollutants that cover the valley and its immediate surrounding areas. The CTM simulation was performed at the horizontal grid resolution of 1 km × 1km. The model was initialize with the gridded emission inventory prepared, WRF simulated meteorological fields and run for the period of 0215 UTC (0800 LST) 7 December to 0215 UTC (0800 LST) 9 December 2018. However, the spatial and temporal distribution of concentration fields were observed on 08 December 2018.

3.5 Other Tools/Software

3.5.1 Geographic Information System (GIS)

GIS is a conceptualized computer based framework that assists to capture, manipulate and analyze spatial and geographic data. It has variety of applications. Thus this technology allow the detail analysis of spatial patterns of various atmospheric parameters in meteorology and climatology. The air pollution dispersion maps of major pollutants having topographical features in 1km×1km grid resolution can also be prepared by this technology. GIS can be handed, visualized in two or three

dimension performing different kinds of mathematical operation and can be used in effective decision making [47]. ESRI's ArcGIS 10.6 software has been used for comprehensive work in GIS for this thesis work. The coordinate system used throughout the study is projected Universal Transverse Mercator (UTM) (WGS 1984 UTM Zone 44N), with false easting 500000 m, central meridian of 81°, scale factor of 0.996 and the geodetic system 'WGS 1984'. Data set of any co-ordinate system is converted to projected co-ordinate system for more accurate calculation. The data management tool "Arc tool box" of GIS, projection and transformation, helps us to convert data in any co-ordinate system into the projected coordinate system. The GIS data source such as terrain elevation data, map sheet data and land use land cover data are freely accessible on internet in proper formats. ESRI's ArcGIS 10.6 has been widely applied for spatial distribution of air pollution hotspots, calculate emission estimation field's calculation, locating gridded distribution of emission fields and visualization and analysis purpose.

3.5.2 The Google Earth Pro

Google map is a useful tool for analyzing, collecting, and recording information of any location. It offers the most comprehensive set of publicly available geospatial data with high resolution, detailed road maps, imagery of various location. The spatial coordinate of transportation, industrial, commercial, residential sectors can be easily investigated on Google Earth and can be imported into the Arc Map for further clarification. In this thesis, we have adopted Google Earth pro for finding location of different Public vehicle route.

Chapter 4
RESULT AND DISCUSSION

4.1 Introduction

It has been described the important findings of result into different section and subsection. At first validation of meteorological fields are validated to the observe data in Kathmandu valley. Furthermore, spatial and temporal characteristics of ambient wind, vertical structure, and wind characteristic, gridded emission inventory of potential pollutants and their implication have been discussed. Finally, findings on air pollution dispersion and formation of pollutant fields by using CTM model over public transport are presented.

4.2 Rationales of the WRF Simulated Meteorological Fields

The section examines the meteorological simulation against the SODAR-RASS field measurements (temperature and winds) recorded at Kirtipur on 8 December 2018.The Figure 4.1 (a-f) presents the simulated and observed diurnal variation of wind speed and temperature at different altitudes (30 m, 90 m and 200 m above the ground level), respectively, the corresponding regression analysis (a'-f'). It can be examined that during late evening (around 2000 LST) to the late morning (around 1100 LST) next day the surface level (from height 30 m AGL to 200m AGL) wind speed generally remains calm. During late afternoon from 1600 LST to 1900 LST windspeed occurs maximum that often reaches 5 m/s but generally remains 3.5 m/s in the central part of the valley. The phenomenon that gradual increase of wind speed begins from noon and reaches maximum at late evening suggest the intrusion of local flows (North-westerly and South-westerly) over the valley. The scattered plots (Figure 4.1, a'-f ') presents regression analysis relative to wind speed and temperature throughout the diurnal variation over 3 days. In case of wind speed, it can be clearly observed that 0.9079, 0.9104, and 0.8965 are the coefficient of determination (R^2) at height 30m, 90m and 200 m,respectively. The higher altitudes (90m and 200m) possess greater wind speed in evening time and is more by 1.6 m/s than that of 30m height. These high winds are caused by downslope wind from surrounding mountain slopes and due to the surface frictional drag the surface wind speed slow down.

Likewise, the Figures 4.1 also shows the WRF simulated and RASS derived diurnal variation of temperature profile above 30m, 90m and 200m AGL in Kirtipur premises dated on period 8 December

2018. Similarly, its associated regression analysis provides the coefficients 0.8467, 0.9246, and 0.8674 respectively. The maximum temperature is recorded at close to 1 pm and is about 15°C. Temperature drops to minimum at close to early morning around 6 am in the morning at 40 m above the ground. Graphically, we can see that the minimum temperature rises as we move greater heights. The coefficient of determination at different heights, 40m 90m and 200 m, are 84.7%, 92.5% and 86.7%.
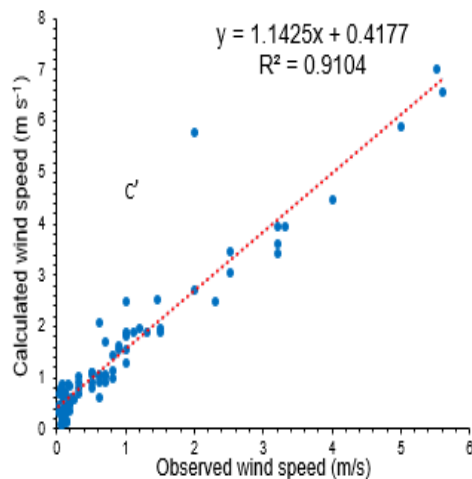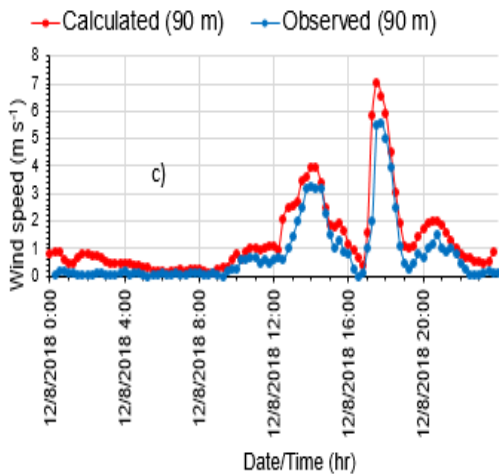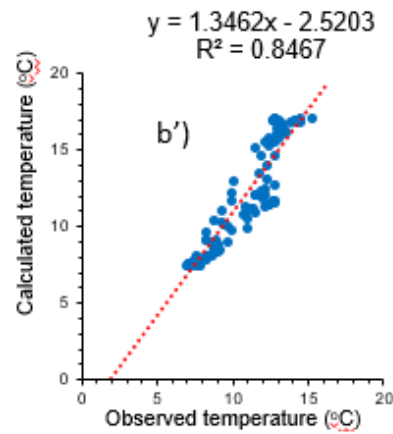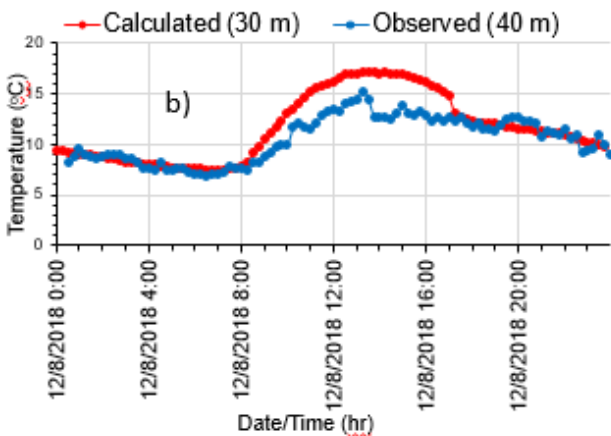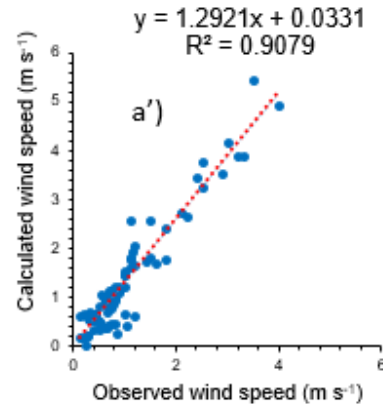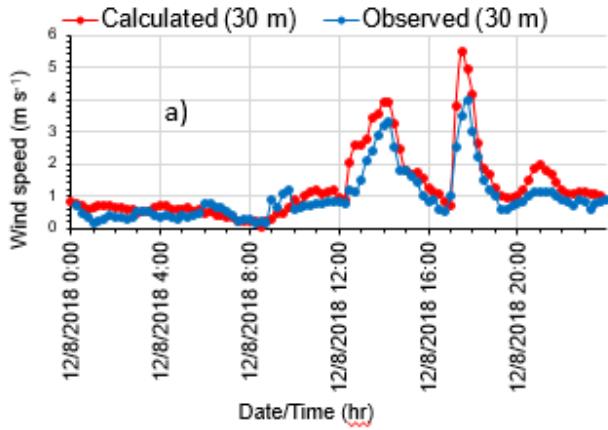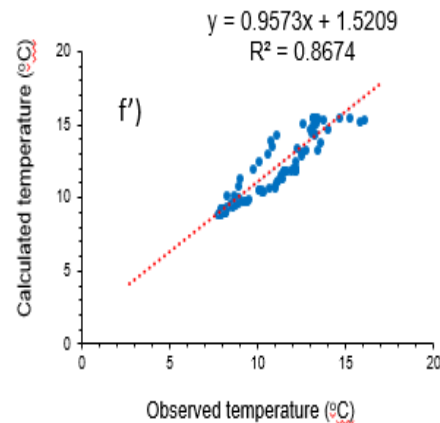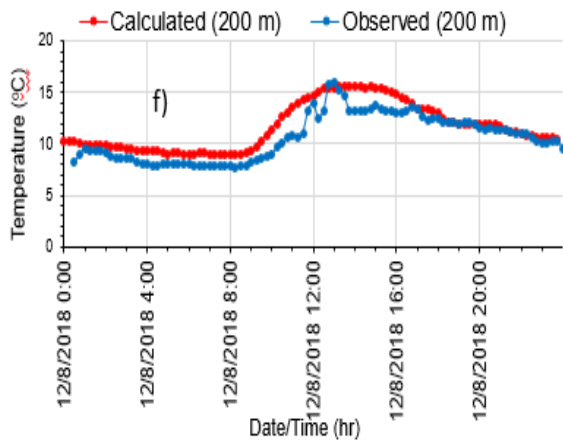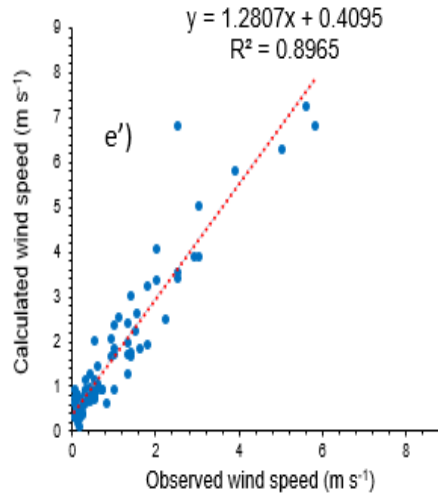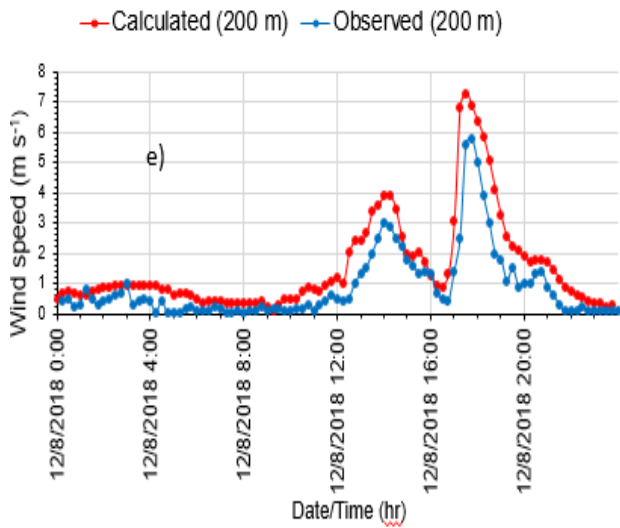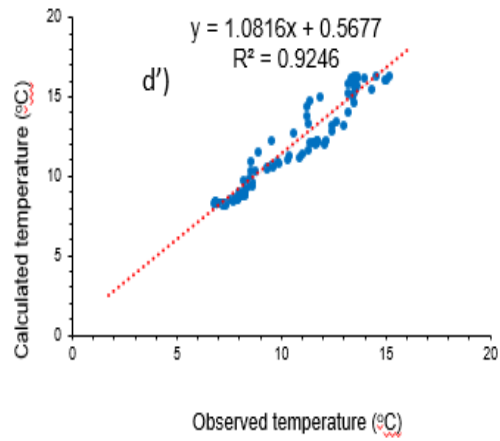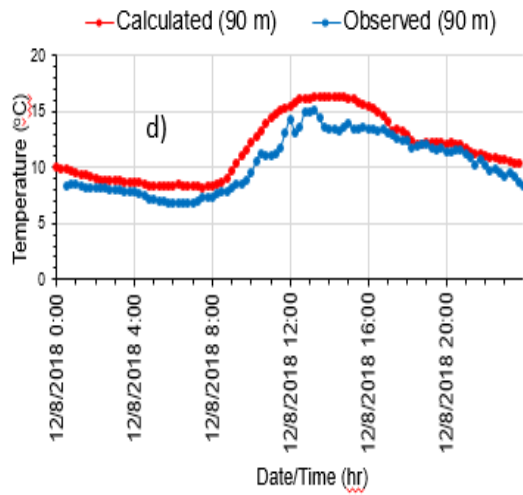
Fig 4.1: Time series of wind speeds (a-c) and temperatures (d-f) from WRF model (Blue), and SODAR-RASS (Red) (Left side plots), Scatter plots within every 15 minutes for wind speed (a'-c') from WRF model and SODAR-RASS, and temperature (d'-f') from WRF model and SODAR-RASS at different representative heights (Right side plots).

From these plots, basic feature of winter time meteorological parameters like temperatures and wind flows over the valley are well resolved in numerical simulation. Thus, the WRF model prediction skill is good as it resemblance well with observations.

4.3 Meteorological flow Characteristics
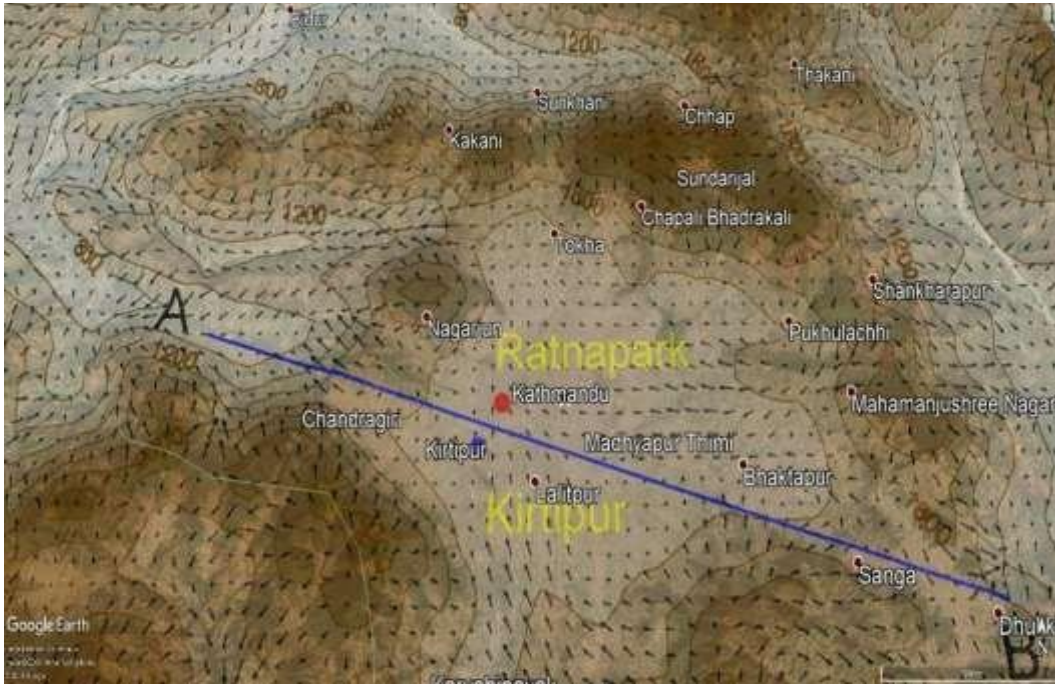
Figure 4.2: Geographical coverage of study area showing important places. Along the line A-B vertical cross-sectional variation of meteorological fields will be discussed.

This section presents the local meteorological flow characteristics in and around the Kathmandu valley. Examining the series of hourly average near surface winds, vertical cross-sectional distribution of potential temperature, vertical and horizontal wind fields (see Figure below), following characteristics can be noticed. The valley floor remains calm or windless during the late evening to late morning. As a result, valley develops very strong surface inversion. The surface inversion begins to erode from the surface around 8 AM and mixing layer height gradually increases beyond 8 AMand reaches to about 1200 m above the valley floor in the afternoon. However, the valley remains capped by strong stable layer at the level of surrounding mountaintops. Two prominent winds, namely, southwesterly and north-westerly intrude into the valley close to the noontime viasouthwesterly river gorge and the western low mountain passes to merge into a westerly over the central area of the valley. The westerly then channel into the eastern neighbouring valley. These winds prevail until the early evening. The speed of near surface wind reaches to about 5 m s^{-1} during the late afternoon.

The meteorological flow fields suggest strong surface inversion during the night and morning strongly suppress the vertical dispersion of pollutants and confine the pollutants within a very shallow layer.

The pollutants released during the period build up a high level of air pollution at the surface level. Erosion of surface inversion and initiation of mixing activities efficiently disperse vertically until the noontime. Intrusion of the southwesterly and the north-westerly winds organize the pollutants transport towards the east and flushes into the eastern neighbouring Banepa valley until the late afternoon. Accumulation of pollutants over the valley floor from the early evening.
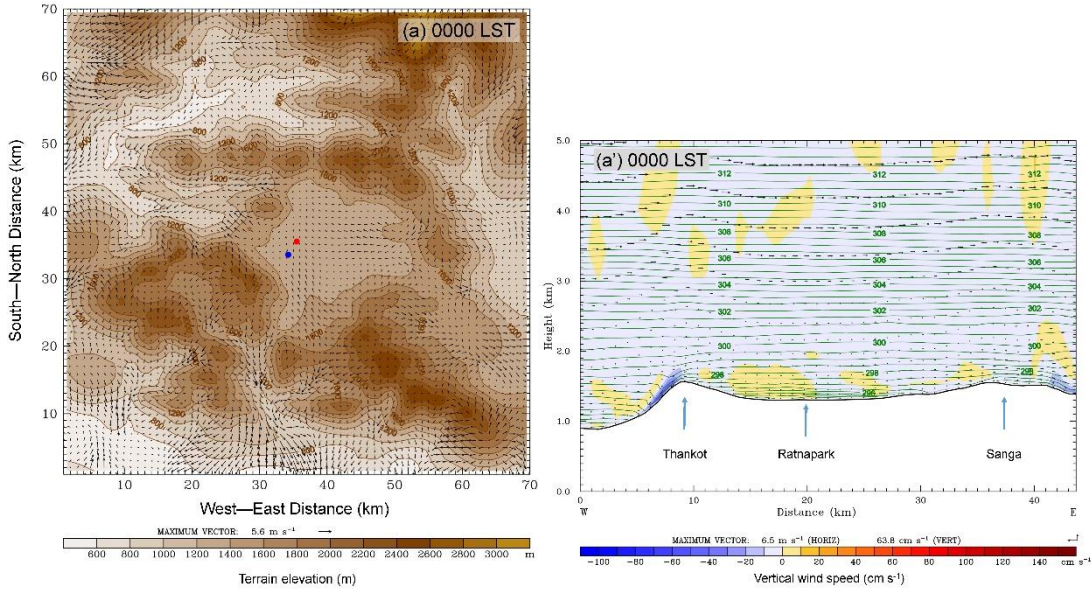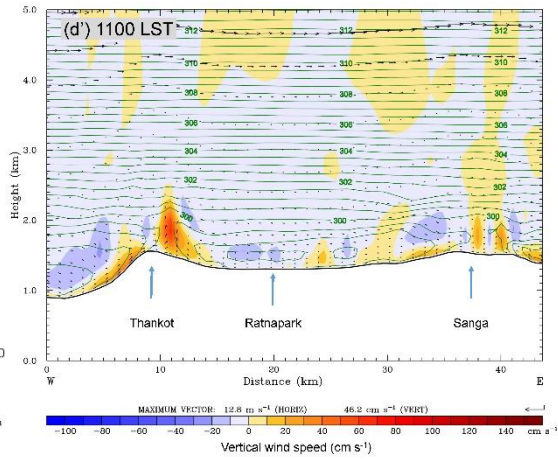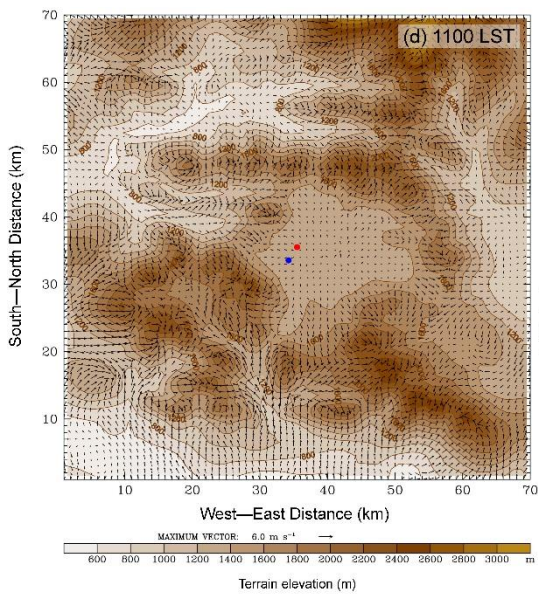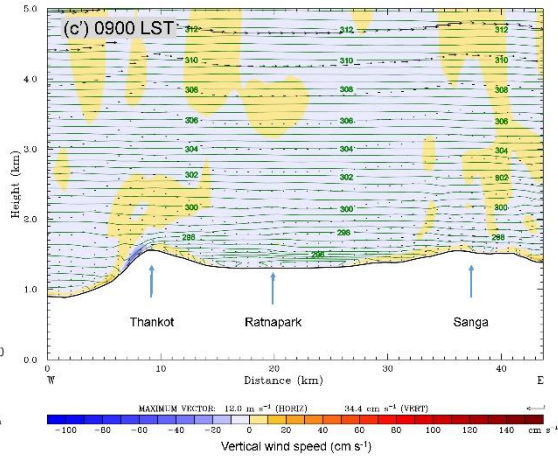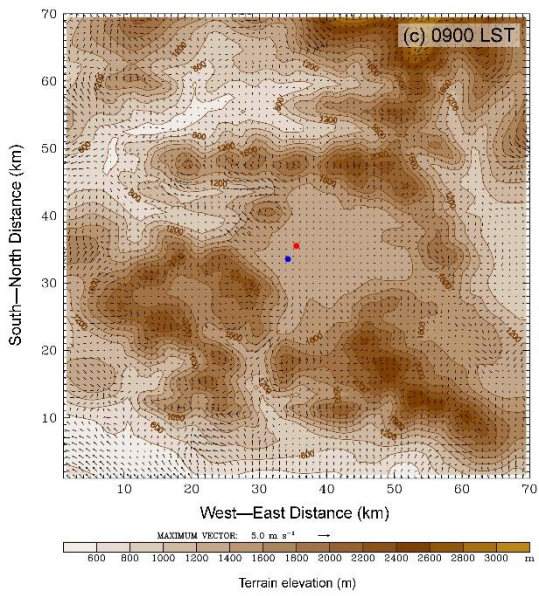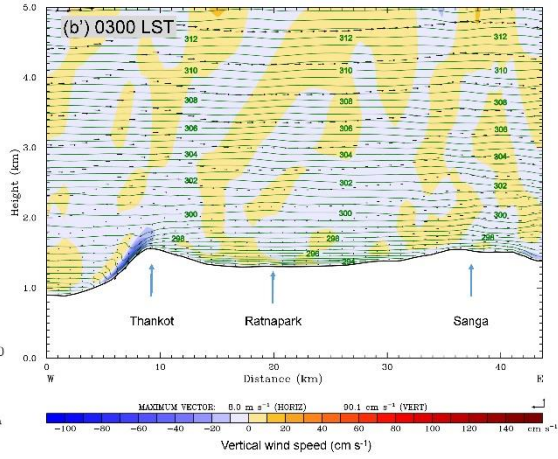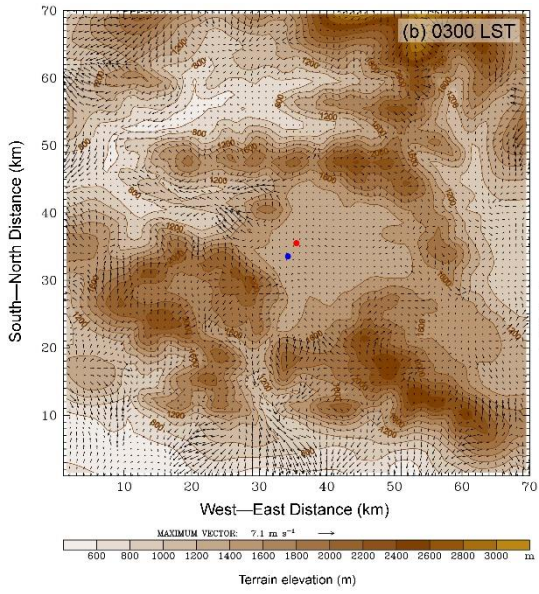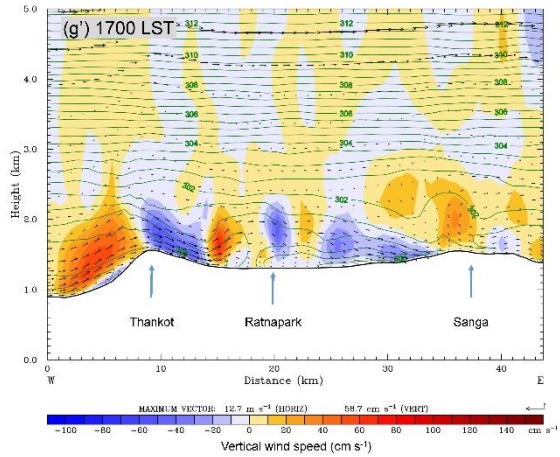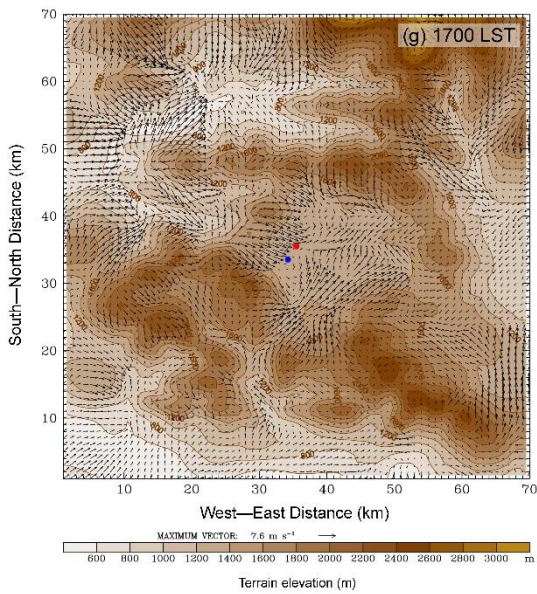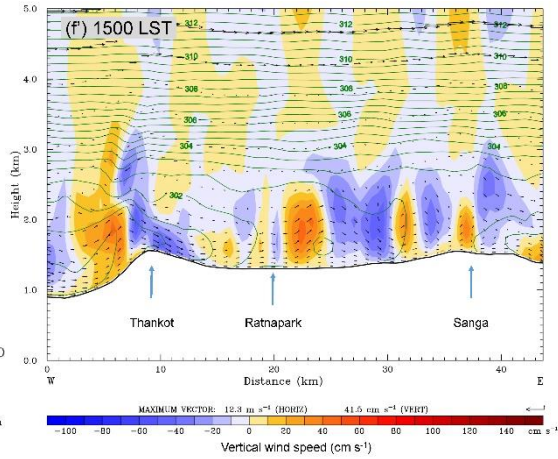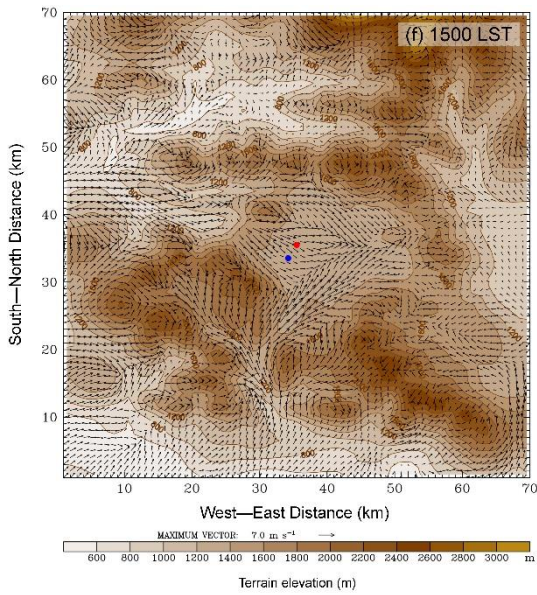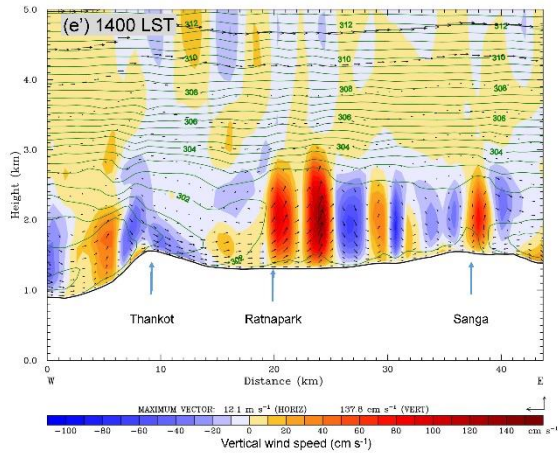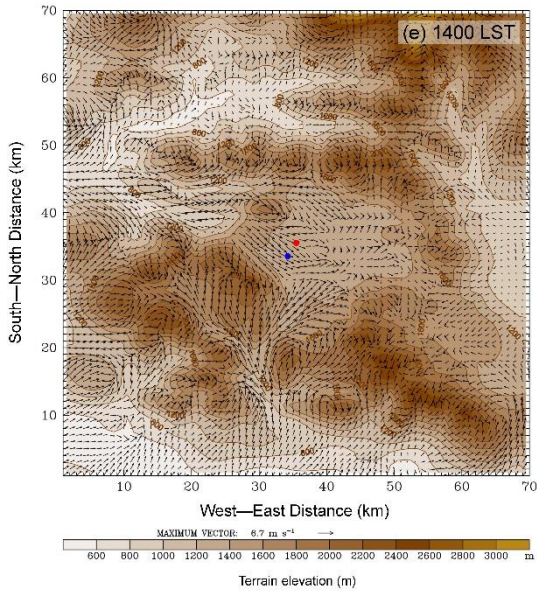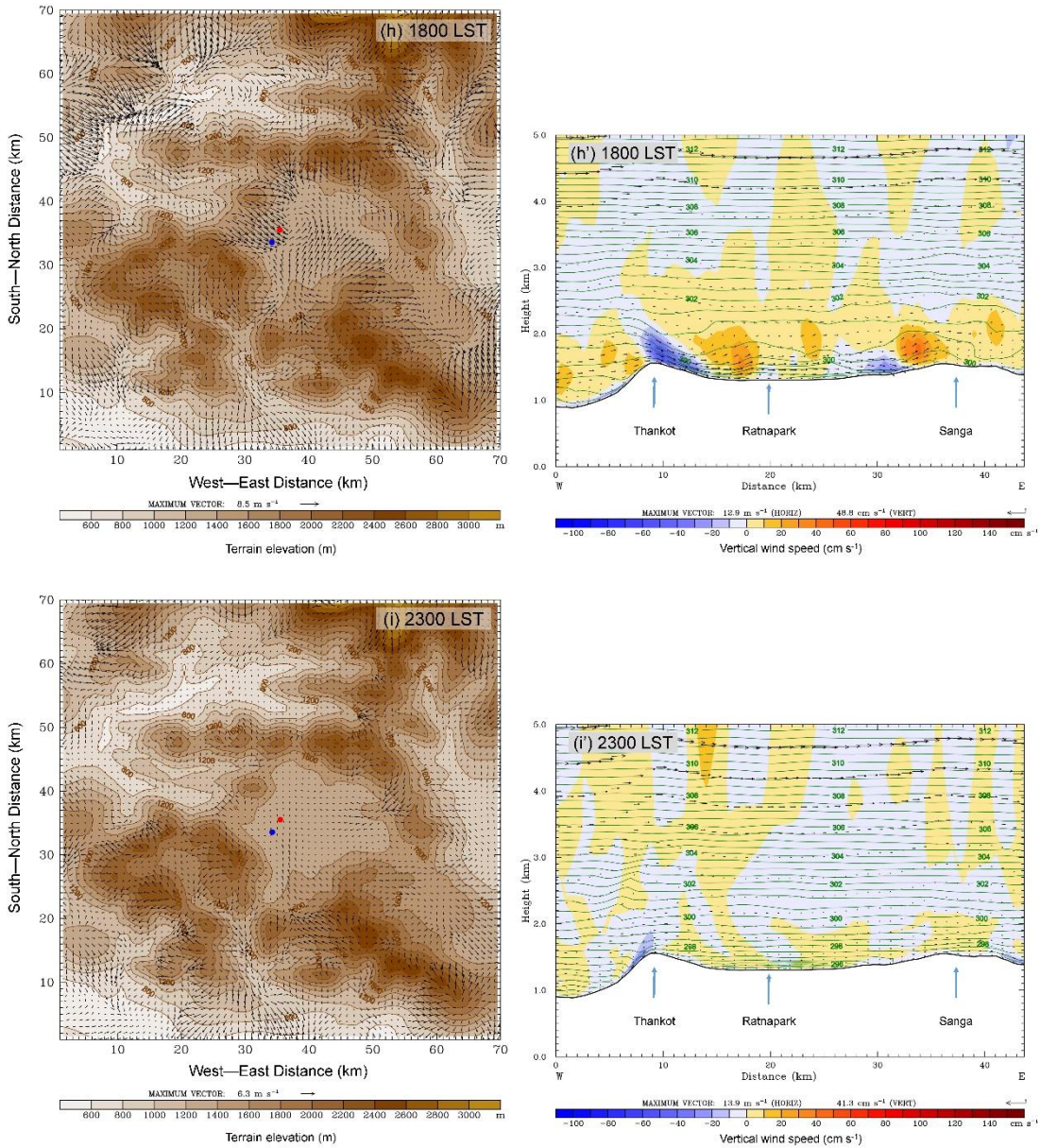
Figure 4.3: Spatiotemporal distribution of near surface winds (vectors) superimposed with terrain(filled contours) (a-i); and, the vertical cross-sectional distribution of horizontal winds (vectors), vertical winds (raster) and the potential temperature (contours) over the valley along the A—B shown in Figure 4.4 (a'-I').

4.4 Gridded Spatial Distribution of Pollutants

Potential pollutants such as oxides of nitrogen (NOx), carbon monoxide (CO), oxides of Sulphur (SOx) and the total suspended particulate matter (TSP) are estimated by using emission factor and fuel used pattern at horizontal grid resolution of 1km x 1km over the area of 70 km x 70 km centered at the centralarea of the valley from the public transport fleet of Kathmandu valley.
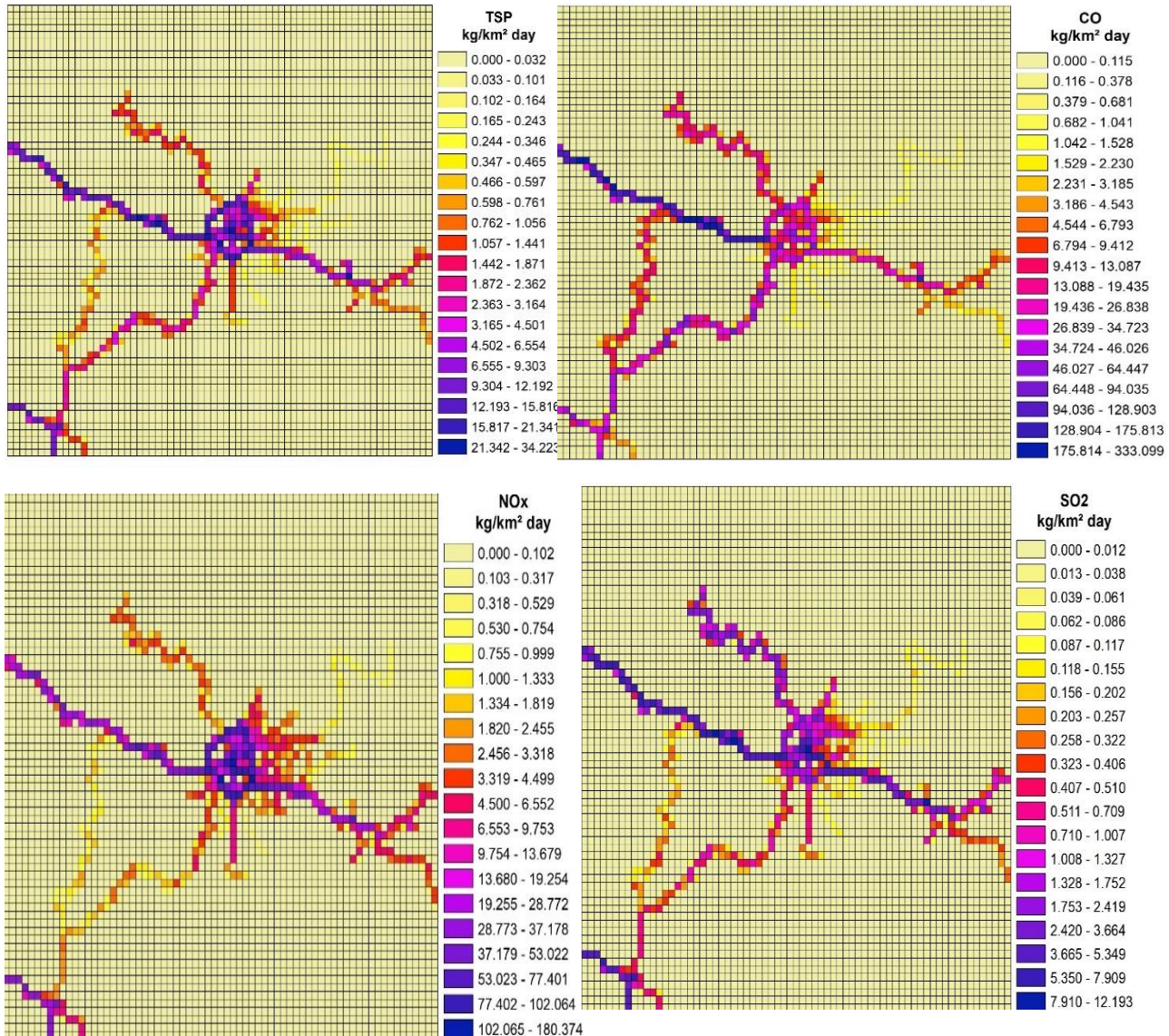

Figure 4.4: Gridded emission field of (a) TSP, (b) CO, (c) NOx, (d) SO2 for public transport of Kathmandu valley. The horizontal grid resolution is at 1km × 1km dimension.

It reveals that the distribution of pollutants emission mostly confines over the central area of the valley namely core city and main road junctions such as Ratnapark, Kalanki, Koteshwor, Satdobato along

with its surrounding periphery. The daily average of emission of TSP, CO, NOx, and SO$_2$ are estimated at 1918.174249, 12872.742169, 6925.816719 and 708.406454 kg, respectively (see Table below).

| Pollutants	Quantity of pollutants kg per day
TSP	1918.174249
CO	12872.742169
NO$_X$	6925.816719
SO$_2$	708.406454
Total	22,425.139591

Table 4.1: Estimated daily average emission of pollutants over the Kathmandu valley during the winter season of 2018 form the public transport fleet.
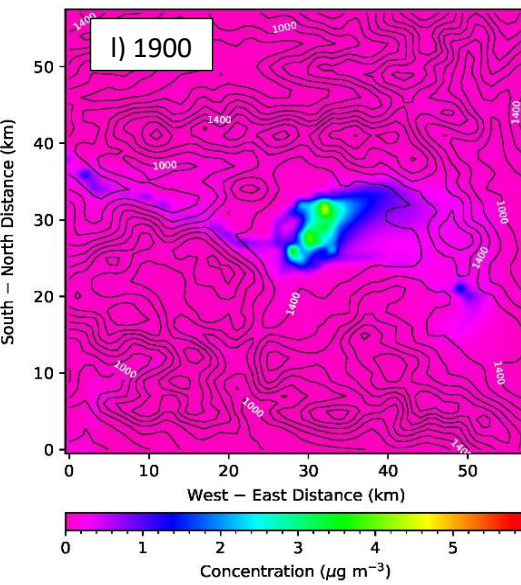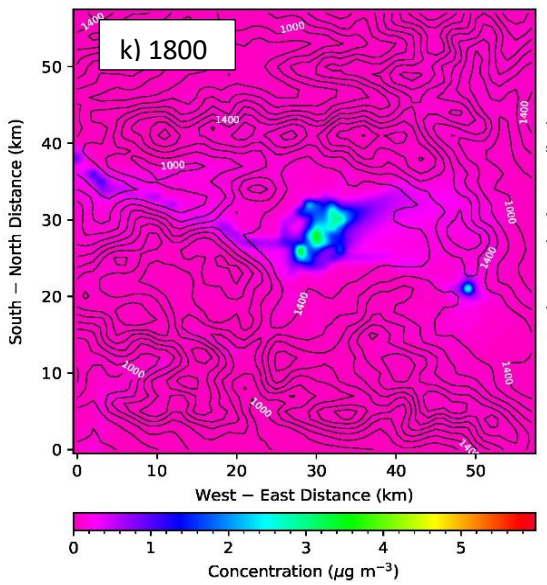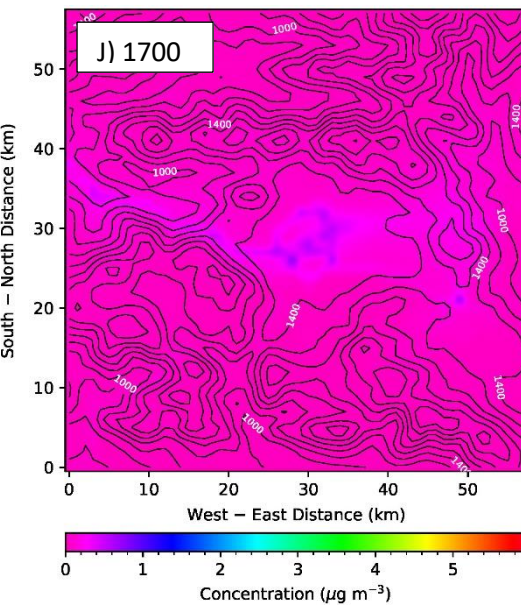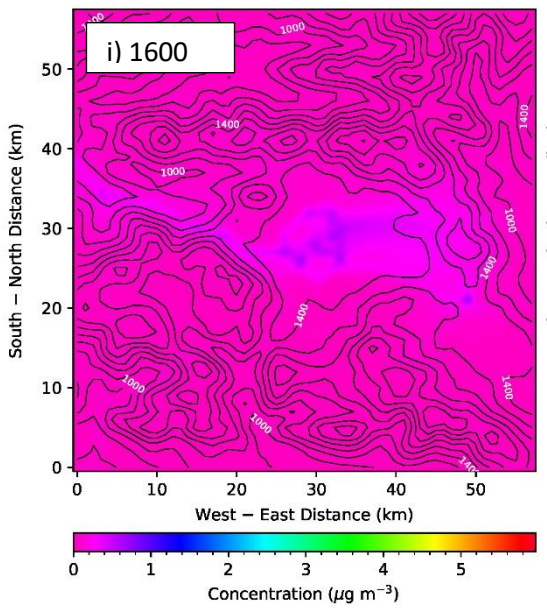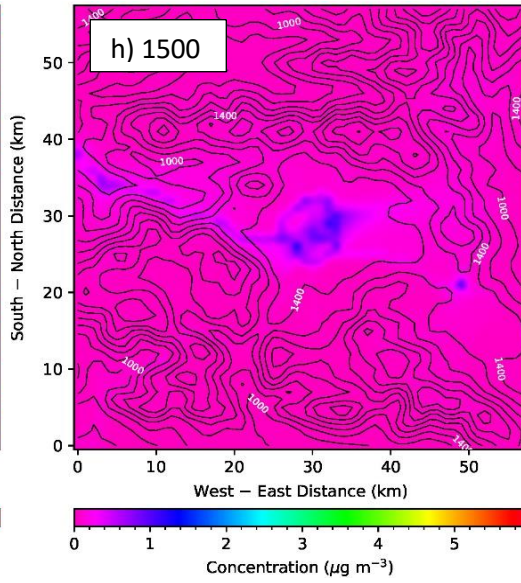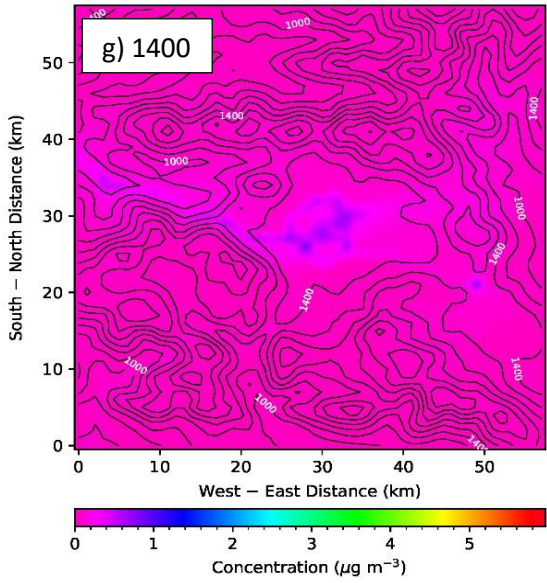
4.5 Spatiotemporal Distribution of Particulate Pollutants

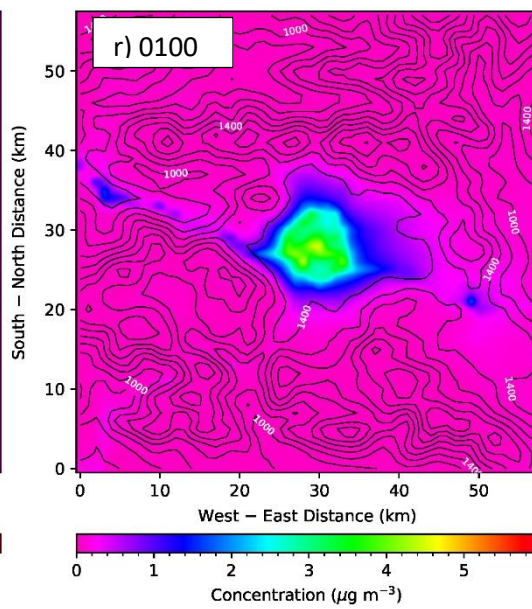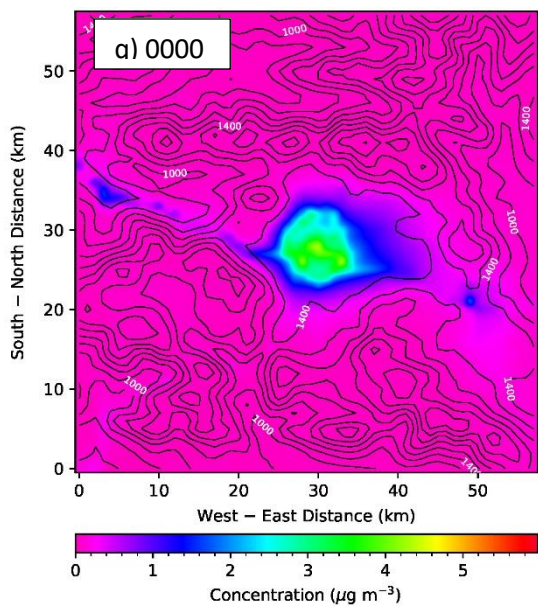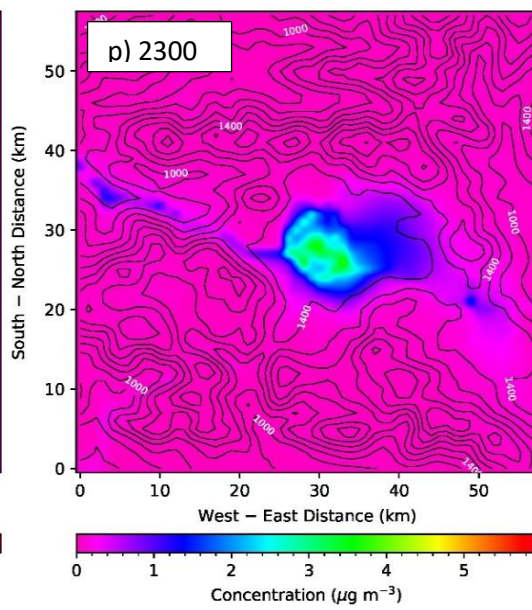The spatial and temporal distribution of PM$_{2.5}$ is often considered as a surrogate measure of pollution has been presented in this section. CTM is used for the study of spatial and temporal distribution of PM$_{2.5}$ was performed for the period of 07 December to 09 December 2018. However, for the discussion of spatiotemporal distribution of pollutants released from the public transport fleet of Kathmandu valley, we consider the day of 08 December 2018 as the representative winter days in Kathmandu.

Figure 4.5 shows surface level spatial and temporal distribution of PM$_{2.5}$ pollutant at surface (2m AGL) over the Kathmandu valley on the specific day of 08 December 2018. As discussed earlier on the meteorological implications for air pollution transport, the pollutants released from the public transport fleet builds up and remains confined over the central part of the valley in a shallow layer can be seen in the Figures (4.5,a-j). The gradual increase in concentration of PM$_{2.5}$ until surface inversion stars to erode around 08 AM. The vertical dispersion of pollutants as well as horizontal spreading the concentration over the central part of the valley decreases with the persistent value beyond 08 AM. Pollutants are transported towards the east and finally flushes into the Banepa valley during the afternoon by Intrusion of southwesterly and northwesterly wind in the afternoon. Soon the regional southwesterly and the northwesterly winds cease in the early evening, the pollutants released over the valley begins to accumulate over the valley floor and gradually returns almost to the same situation

described earlier for morning time distribution. This shows that there prevails a strong diurnal periodicity in the transport of pollutants over the Kathmandu valley during the winter season.
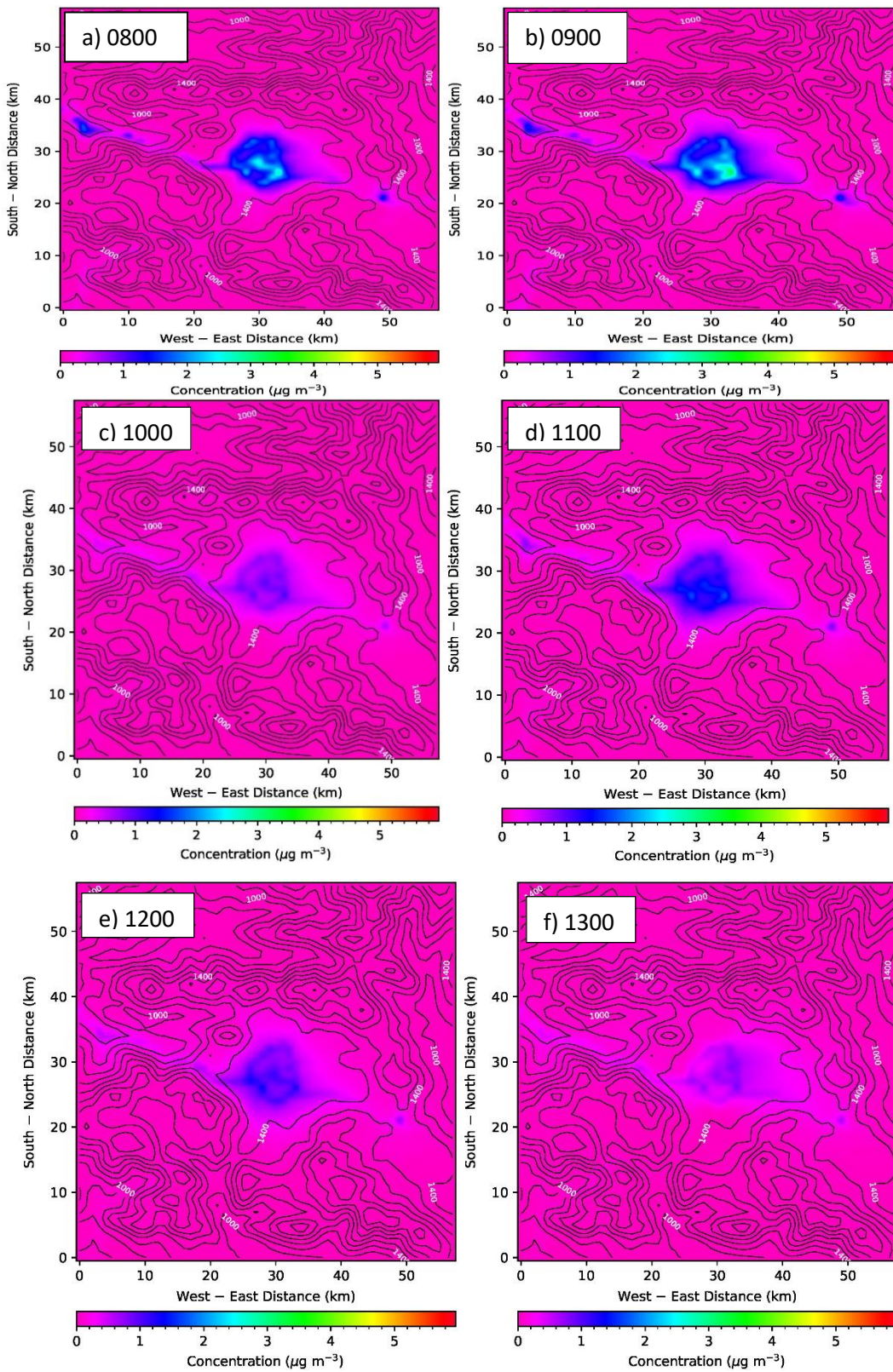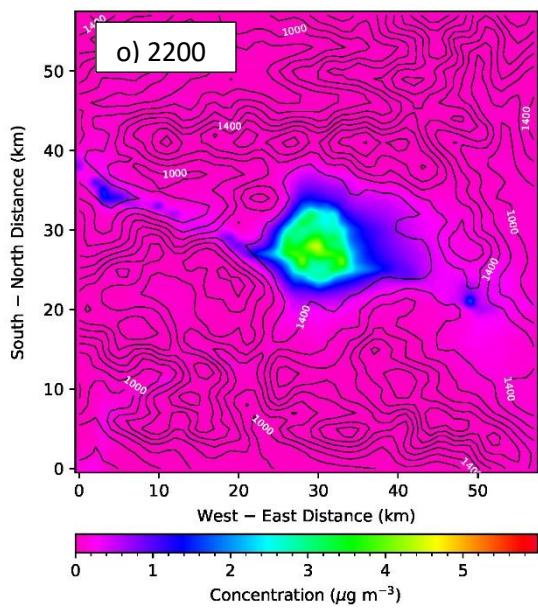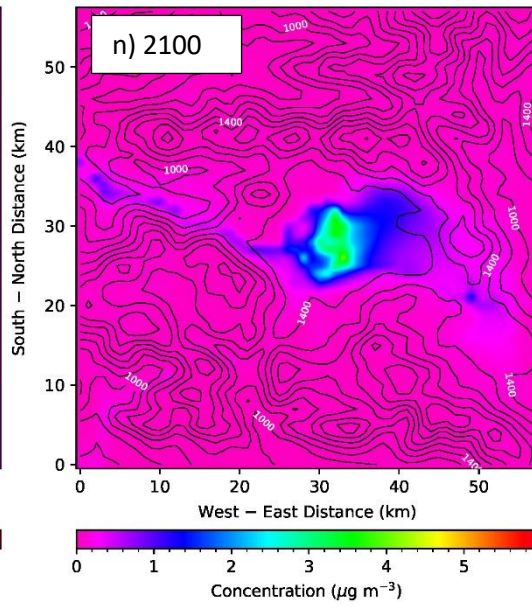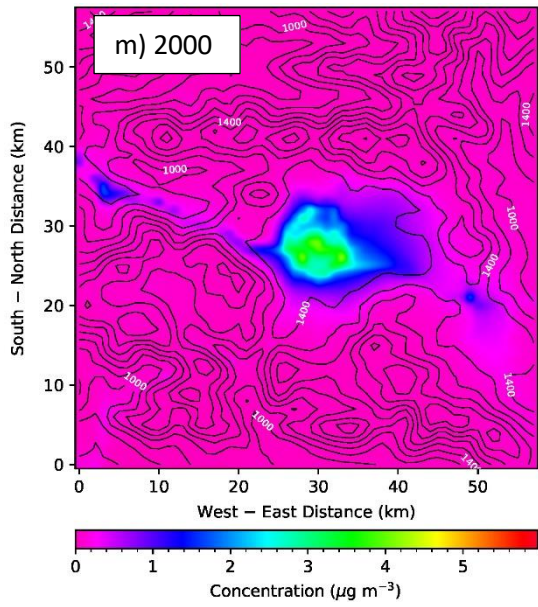
Figure 4.5: Spatiotemporal distribution of PM$_{2.5}$ pollutants in and around the Kathmandu valley released from the public transport fleet.

Chapter 5

CONCLUSIONS AND RECOMMENDATIONS
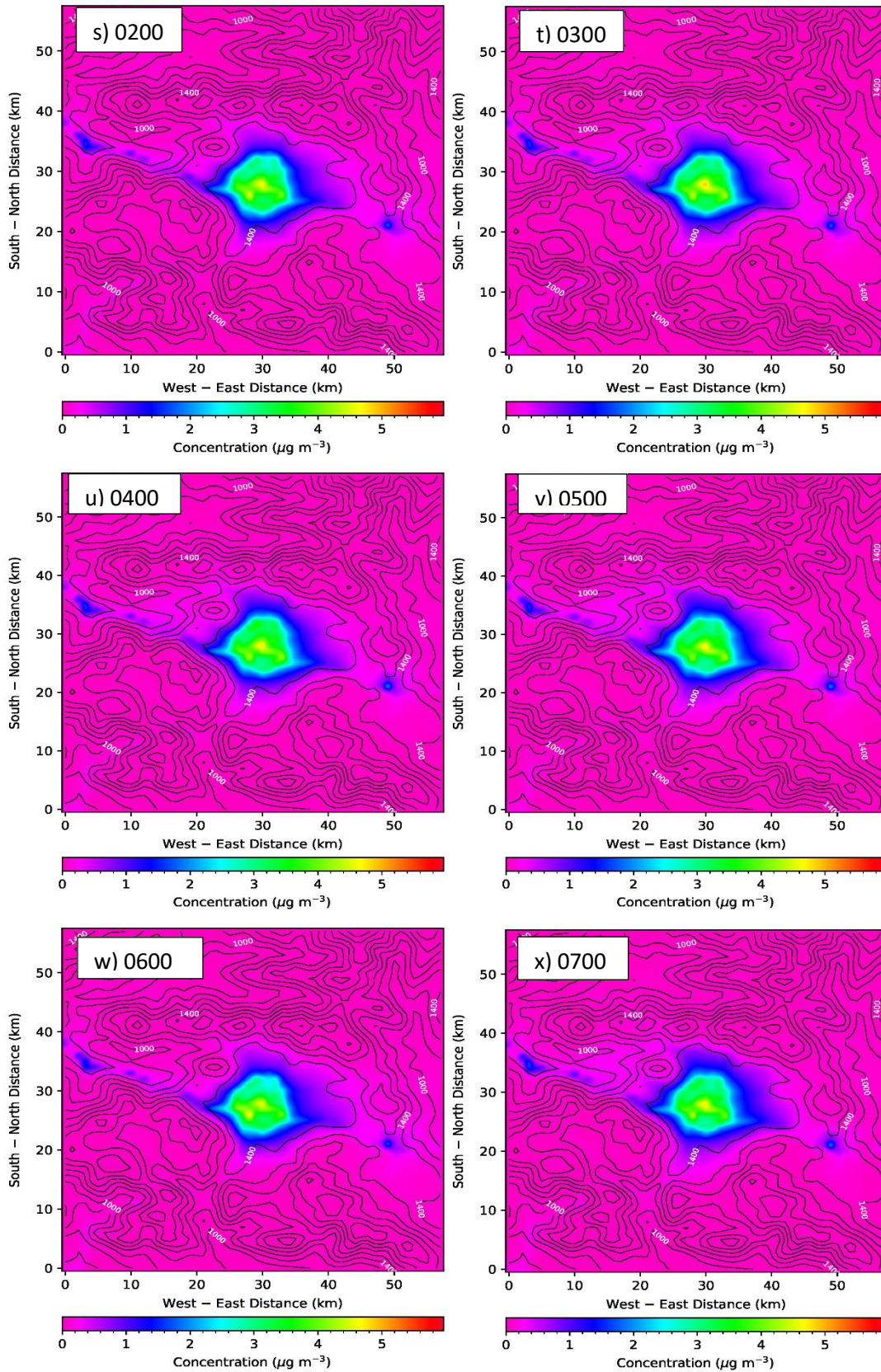
5 Conclusions and Recommendations

The study was achieved to gain knowledge the meteorological implications for air pollution transport,spatial distribution of emission loadings from public transport fleet and the dispersion pattern of pollutants over the bowl shape valley viz. Kathmandu valley, was realized by conducting the numerical simulation of meteorological flow fields using the WRF modeling system, preparing the gridded emission inventory from secondary data, and the CTM modeling. The WRF prediction skill is tested against the sodar-rass derived winds and temperature profiles. A reasonably well agreement in between the WRF simulated and sodar-rass derived wind and temperature profiles noticed that the simulated meteorological parameter were representative.

The WRF simulation shows the Kathmandu valley consists a very poor airpollution dispersive power. The atmosphere closed to the surface of the valley remains clam under strong thermal inversion, trapping the pollutants in a thin layer. Two major gentle winds, namely, the southwesterly and northwesterly blow the valley floor from noon to early evening and are responsible to flush out pollutant from the valley

The gridded emission estimation of public vehicle fleet states that emission from public transport is confined within the city areas enclosed by the Ring Road of the Kathmandu valley. The average emissions of TSP, CO, NOx, and SOx are estimated at 1918.17, 12872.74, 6925.82 and 708.41 kg per day, respectively. The CTM simulated spatiotemporal $PM_{2.5}$ pollutant over the bowl-shaped valley viz. Kathmandu valley suggests that the pollutants revealed from the public transport fleet spread and residue restricted over the central part of the valley in a surface layer during the night and morning until the nighttime surface inversion begin to erode around 8:00 AM. The nighttime stationary pollutants over the valley dispersed vertically and spread horizontally with beginning of mixing activities beyond 8:00AM. Disturbance of southwesterly and northwesterly wind in the afternoon blow the valley floor by ambulant the pollutants towards the east and glowing into the eastern valley via the eastern low-mountain passes.The pollutants revealed over the valley begins to build up over the valley floor and rapidly yields to the early morning situation next day representing a strong diurnal periodicity in the meteorological flows and pollutant transport over

55

the valley during the winter days of Kathmandu. Contribution of emission from the new system having public transport fleet in the improvement of air quality appears quite low compared to the other old model's public transport at present but it is probable to increase rapidly in future due to increasing number of public transports. In reference to present observation and findings related to air pollution scenario by public transport over the valley, some of the recommendations to minimized air pollutions by public transport are as follows:

- Government should strictly implement the polices regarding pollution controlling transportation system and replacement of high polluting transport viz. old transport with new transport.

- Transportation having fuel engine system should be replaced with electric engine system.

- Long term numerical simulation and emission inventories on air pollution transport process over the major urban centres of Nepal with extensive field observations is also recommended for future studies

Chapter 6
LIMITATION OF STUDY

6 Limitation of study

The outcomes of this study are based on the analysis of short-term simulation over winter time. So, day-to-day variation in wind flow patterns are likely to occur. Likewise, emission estimation is targeted for winter time only so it may not give proper emission information at rest of the season. Thus, present study lacks to account the seasonal variations in the meteorological characteristics and emission information. Besides, large numbers of private vehicles are operating every day and its contributions are not considered in this study. On considering both private and public vehicles, the emission map and dispersion map are likely to be different than present. Extensive measurements are highly desired to understand the natural processes in our surrounding and to understand the advantage and disadvantage of the numerical weather prediction model as well.

REFERENCES

[1] http://www.cen.org.np/uploaded/ (viewed on 23 November 2018).

[2] Public Bus Accessibility and its Implications in Energy and Environment: A Case Study of Kathmandu Valley

[3] http//www.kantipuronline.com

[4] R. P. Regmi, T. Kitada and G. Kurata, J. Appl. Metero., **42,** 389-403 (2003).

[5] Central Bureau of statistics. Environmental statistics of Nepal 2019; Government of Nepal: Kathmandu, Nepal (2019).

[6] B. Sapkota and R. Dhaubadel, **36**, 1249-1257 (2002).

[7] R. P. Regmi, T. Kitada, G. Gross, G.C. Kafle, S. Maharjan, S. Shrestha, A.K. Khadka, S. Adhikari, National Atmospheric Resource and Environmental Research Laboratory (NARERL), Tribhuvan University, Kirtipur (2018).

[8] R. P. Regmi, T. Kitada and G Kurata, J. Appl. Meteor., **42**, 389-403 (2003).

[9] R. M. Shrestha, *Emission of Air pollutants and Greenhouse Gases in Nepal,* Thailand (2018).

[10] T. Kitada, and R. P. Regmi, J. Appl. Meteorol., **42**, 1770-1798, (2003).

[11] S.R. Shrestha, N. T. K. Oanh, Q. Xu, M. Rupakheti, M, G. Lawrence, Atmos. Environ., **81**, 579-590 (2013).

[12] WHO, *WHO Air quality guidelines for particulate matter, ozone, nitrogen dioxide and sulphur dioxide, Global update 2005, 1-22,* (2006).

[13] National Ambient Air Quality Standard, 2012, Department of Environment, Nepal (2012).

[14] Y. F. Xing, Y. H. Xu, M. H. Shi, and Y. X. Lian, Journal of thoracic disease, 8, E69–E74 (2016).

[15] C.K. Sharma, Atmos. Environ., **31**, 2877-2883 (1997).

[16] S.R. Devkota, UNDP/Nepal, Report No. 92-034 (1993).

[17] I. L. Shrestha, and S.L. Shrestha, Int. I. Occup., **11**, 150-160 (2005).

[18] S. L. Shrestha, Int. J. Environment and Pollution, **27**, 359-372 (2006).

[19] J. M. Wallace, and P.V. Hobbs, Atmospheric Science, Elsevier, Canada (2006).

[20] M. L. Salby, Fundamental of Atmospheric Physics, Academic Press, Cambridge (1996).

[21] C. D. Whitemann, Mountain Meteorology, Oxford University Press, New York (2000).

[22] J. R. Garratt , Earth Science Reviews, **37(1994)**, 89-134, (1994).

[23] R. B. Stull, *An Introduction to Boundary Layer Meteorology,* P. **667**, Kluwer Academic Publishers, Dordrecht/Boston/London (1989)

[24] S. Emeis, *Surface-Based Remote Sensing of the Atmospheric Boundary Layer,* Vol. 40, p. **171** Springer, Netherlands (2011)

[25] http://www.archaeocomology.org/eng/tropospherelayers.htm (Viewed on July 7, 2019)

[26] J. M. Marshall, A. M. Peterson, and A. A. Barnes, Appl. Opt. **11,** 108 (1972).

[27] D. A. M. Engelbart, and J. Bange, Theor, Appl. Climatol **73**, 53 (2002).

[28] http://www.google.com/earth/ (Viewed on June 22, 2019).

[29] R. M. Shrestha, N. T. K. Oanh, R. P. Shrestha, M. Rupakheti, S. Rajbhandari, D. A. Permadi, T. Kanabkaew, and M. Iyngararasan, *Atmospheric Brown Clouds (ABC) Emission Inventory Manual,* United Nations Environment Programme, Nairobi, Kenya (2013).

 [30] W. C. Skamarock, J. B. Klemp, J. Dudhia, D.O. Gill, D. M. Barker, M. Duda, X.-Y. Huang, W. Wang, and J. G. Powers, *A description of the Advanced Research WRF version 3. NCAR Technical Note*, NCAR/ TN-475+STR, (2008).

[31] R. P. Regmi, and S. Maharjan, *Trapped mountain wave excitations over the Kathmandu valley, Nepal*, Asia-Pacific J Atmos Sci, **51**, 303–309 (2015).

[32] R. P. Regmi, T. Kitada, J. Dudhia, and S. Maharjan, *Large-scale gravity current over the middle hills of the Nepal Himalaya: Implications for aircraft accidents*, J. Appl. Meteor. Climatol. **56**, 371–390 (2017).

[33] J. B. Klemp, W. C. Skamarock, and J. Dudhia., *Conservative split-explicit time integration methods for the compressible no hydrostatic equations*, Mon. Wea. Rev., **135**, 2897-2913 (2007).

[34] W. C. Skamarock and J. B. Klemp, *A time-split no hydrostatic atmospheric model for weather research and forecasting applications*, J. Computational Phys., **227**, 3465-3485 (2008).

[35] WRF-ARW Version 3, Modelling System User's Guide, Mesoscale and microscale meteorology division, National Centre for Atmospheric Research (2013).

[36] R. Laprise, *The Euler Equations of motion with hydrostatic pressure as independent variable*, Mon. Wea. Rev., **120**, 197–207 (1992).

[37] W. C. Skamarock, J. B. Klemp, J. Dudhia, D. O. Gill, D. M. Barker, M. Duda, X. Y. Huang, W. Wang, and J. G. Powers, *A Description of the Advanced Research WRF Version 3*, (No. NCAR/TN-475+STR), (2008). doi: 10.5065/D68S4MVH

[38] F. M. Ralph, C. Mazaudier, M. Crochet, and S. V. Venkateswaran, *Doppler Sodar and Radar Wind-Profiler Observations of Gravity-Wave Activity Associated with a Gravity Current,* Mon. Wea. Rev., **121**, 444–463 (1993).

[39] T. Kataoka, M. Takehisa, Y. Ito, and Y. Mitsuta, *A low Level Jet Observed by a Doppler Sodar during the International Sodar Inter comparison Experiment (ISIE)*, J. Meteor. Soc. Japan, **69**, 171–177 (1991).

[40] V. Kotroni, Y. Lemaitre, and M. Petitdidier*, Dynamics of a low-level jet observed during the Fronts 87 experiment.* Quart. J. Roy. Meteor. Soc., **60**, 277–303 (1994).

[41] Z. I. Janjic, *Nonsingular Implementation of the Mellor- Yamada level 2.5 Scheme in the NCEP Mesoscale Model*, Office Note 437, NOAA/NWS/NCEP, 61 pp (2001).

[42] T. Kitada, G.R.C. Michael, L. K. Peters, *Numerical Simulation of Transport of the Chemically Reactive Species under Land- and Sea Breeze Circulation,* J. Climate APPl. Meteor., **23**, 1153-1172 (1984).

[43] T. Kitada, P. C. S. Lee, and H. Ueda*, Numerical modelling of long-range transport of acidic species in association with meso-β- convective-clouds across the Japan sea resulting in acid snow over coastal Japan—I. model description and qualitative verifications,* Atmospheric Environment, **27A**, 1061-1076 (1993).

[44] G. R. Carmichael, L. K. Peters, and T. Kitada, *A second generation model for regional- scale transport/chemistry/deposition*, Atmospheric Environment, **20,** 1, 173-188, (1986).

[45] G. J. McRae, W. R. Goodin, and J. H. Seinfeld, *Numerical solution of the atmospheric diffusion equation for chemically reacting flows*, J. Comput.Phys., **45**, 1-42 (1982).

[46] T. Kitada, G. R. Carmichael, and L. K. Peters*, The Locally One-Dimensional, Finite Element Method (LOD-FEM) for atmospheric transport/chemistry calculations*, P. Lascaux, Ed., Pluralis, **1,** 223–233 (1983).

[47] O. Huisman and R. A. Deby, *Principle of Geographic Information Systems*, ITC, Enschede, the Netherlands (2009).

APPENDIX

National Atmospheric Resource and Environmental Research Laboratory

(NARERL)

Central Department of Physics

Tribhuvan University, Kathmandu

Survey Questionnaire of Public Transport

Name: …………………………………………………

Address: ……………………………………………

Mobile no.: …………………………………………

[1] What type of fuel used in Public transport? (Tick the suitable option)

| | Diesel | | Electricity |

| | Petrol | | Kerosene |

| | Other |

[2] What types of fuel consume annually?

S. N.	Type of fuel	Amount (kg or ltr/year)	Purpose	Remarks
1	E.g. Diesel	20,000 ltr per year	Transportation	
2				
3				

For any inquiry or information,

you may send email

(shresthachiran540@gamil.com).

Thank you.